

ABSTRACT

HONARI, HAMED. Density Filtering for a Flame-Embedding Approach Based on Large-Eddy Simulation and the One-Dimensional Turbulence Model. (Under the direction of Dr.Tarek Echehki).

The complex nature of turbulent combustion flows requires simulation and modeling of diverse scales. An approach to capturing the inherent multi-scale physics of the combustion phenomena is introduced by the present flame-embedding approach. The approach represents a multi-scale Large-Eddy Simulation (LES) framework used for turbulent combustion. The large-scale grid and LES model account for the low-resolution physics of the flow whereas the fine-scale phenomena, including chemistry, subgrid scale transport, are captured by the One-Dimensional Turbulence (ODT) model.

In Lagrangian LES-ODT, ODT elements are attached to the flame surface and transported along with the flow. Due to the coupling between the two solutions, variables such as velocity and mixture fraction are passed from LES to ODT; while, the ODT density is passed from ODT grids to LES grids. Density fields filtered from ODT solutions are calculated. An approach is proposed to spatially-filter the ODT density to the LES cell centers where there is a flame. The spatially filtered LES density is blended with density solution where only pure mixing is present to obtain a density for LES cells throughout the computational domain.

© Copyright 2013 by Hamed Honari

All Rights Reserved

Density Filtering for a Flame-Embedding Approach Based on Large-Eddy Simulation and
the One-Dimensional Turbulence Model

by
Hamed Honari

A thesis submitted to the Graduate Faculty of
North Carolina State University
in partial fulfillment of the
requirements for the degree of
Master of Science

Mechanical Engineering

Raleigh, North Carolina

2013

APPROVED BY:

Dr. Stephen Terry
Committee Member

Dr. Alina Duca
Committee Member

Dr. Tarek Echehki
Committee Chair, Advisor

DEDICATION

I would like to dedicate my thesis to my parents, professors and advisors who have helped and supported me along the way with their effort, guidance, patience and passion.

BIOGRAPHY

Hamed Honari was born in Tehran, Iran. He started his undergraduate studies in Mechanical Engineering Program at University of Tehran. He conducted his research in the Laser Diagnostic Laboratory (Interferometry and Holography) at the faculty center. After his undergraduate studies, he started working as an engineer at a consultant engineering company to gain experience and enrich his academic studies with practical and industrial projects. Following that, he was admitted the Mechanical and Aerospace Department at North Carolina State University in pursuit of a Master of Science degree.

ACKNOWLEDGMENTS

I would like to thank my advisor Dr. Tarek Echehki for his resolute dedication, wisdom, encouragement and patience he has contributed to my studies at North Carolina State University. He has provided me with his assistance, guidance and expertise.

I am also indebted to my committee members, Dr. Alina Duca and Dr. Stephen D. Terry, who took the time and effort to serve as my committee members and for their valuable feedback. I would also like to express my acknowledgement of their patience, guidance and passion. I feel extremely privileged to have been their student at NC State University.

I would like to thank my lab-mates and friends; Hessam, Fu, Andreas, Sami and Dileep from the Energy Sciences Lab. I would like to thank Sumit Sedhai for the help and advice on his code.

I would like to express my gratitude to my parents, brother, and my family who supported me with their never-ending love. It would not have been possible without their encouragement, sacrifices, advice and guidance throughout my life. I would like to dedicate my thesis to them. They have inspired me to strive for excellence and have stood by my side throughout the highs and lows of my endeavor.

TABLE OF CONTENTS

LIST OF TABLES	vii
LIST OF FIGURES	viii
CHAPTER 1 Introduction	1
1.1 Background	1
1.2 Motivation	3
1.3 Objective	4
1.4 Chapters Outline.....	5
CHAPTER 2 One-Dimensional Turbulence	6
2.1 Introduction	6
2.2 Governing Equations.....	7
2.3 ODT Scalars Calculation.....	9
2.3.1 Density	10
2.3.2 Mass Diffusivity.....	10
2.3.3 Gaseous Mixture Viscosity	11
2.3.4 Specific Heat Capacity.....	12
2.3.5 Thermal Conductivity	12
2.3.6 Mass Production Rate	13
CHAPTER 3 Large-Eddy Simulation and Fire Dynamics Simulator	14
3.1 Introduction	14
3.2 Large-Eddy Simulation	14
3.2.1 Filtering.....	15
3.2.2 Governing Equations	16
3.2.3 Closure	18
3.3 Fire Dynamics Simulator.....	19
3.3.1 Features and Assumptions	20
3.3.2 Hydrodynamic Model	20
3.3.3 Radiation Transport	20
3.3.4 Combustion Model.....	21
CHAPTER 4 LES-ODT Model and Implementation	26
4.1 LES-ODT Framework and Passing Information.....	26
CHAPTER 5 Density Filtering Procedure	29
5.1 Overview	29
5.2 Spatial Filtering (Upscaling)	30
5.2.1 The Gaussian Cubature Method.....	32
5.2.2 Influence Domain and Effective Radius	34
5.2.3 Smoothing of the Filtered Density.....	36

CHAPTER 6 LES-ODT Simulation: Non-Premixed Propane –Air Jet Flame	41
6.1 Objectives.....	41
6.2 Simulation Conditions.....	41
6.2.1 Governing Equations for LES-ODT Flame-Embedding Approach.....	42
6.2.2 Boundary Conditions and Geometry	44
6.2.3 Model Implementation.....	45
6.3 Results	48
CHAPTER 7 Conclusion and Future Work	54
7.1 Conclusion.....	53
7.2 Future Work	53
REFERENCES	55
APPENDICES	56
Appendix A	60
Appendix B.....	62

LIST OF TABLES

Table 6.1	Simulation Conditions for Non-premixed turbulent flame.....	44
-----------	---	----

LIST OF FIGURES

Figure 3.1	State relations for propane	23
Figure 3.2	Oxygen-temperature phase space presenting where combustion is allowed or not allowed to take place.....	23
Figure 4.1	Coupling of LES with ODT and passing information between two solvers ..	27
Figure 5.1	A schematic illustration of LES-ODT computational grid	31
Figure 5.2.a	The LES cell and ODT element attached to the flame surface in 3D.....	34
Figure 5.2.b	The relative positions of the ODT grid point and LES cell in influenced region	34
Figure 5.3.a	Effective domain adopted for filtering.....	35
Figure 5.3.b	Effective domain oriented in the direction normal to the flame surface.....	35
Figure 5.4	Blending pure mixing solution and filtered density based on ODT solution ..	37
Figure 5.5	Smoothing function used for blending the density from LES-ODT and pure mixing solution	39
Figure 5.6	Flow chart of proposed spatially filtering density for LES-ODT	40
Figure 6.1	A schematic of the computational domain.....	45
Figure 6.2.a	Growth of the flame brush and attached ODT elements at simulation time of 0.18s.....	49
Figure 6.2.b	Growth of the flame brush and attached ODT elements at simulation time of 0.20s.....	49
Figure 6.3	Contribution of the ODT domains to each LES cell in filtering process.....	49
Figure 6.4	Overlapping ODT elements on NCWF contour ($\varepsilon_{i,j,k}$).....	50
Figure 6.5	Temperature field at solution time step of 590	51
Figure 6.6	Temperature field at solution time step of 650	51
Figure 6.7	FDS density field	52
Figure 6.8	Filtered density.....	52
Figure 6.9	Temperature field at 22s	53
Figure A.1	Tri-Linear interpolation for a cell	60
Figure B.1	Finding distance between LES cell center and ODT element	62

CHAPTER 1

Introduction

1.1. Background

Nowadays, combustion is perceived as an applied and practical science in industry. From internal combustion engines in car industry to power plants and industrial processes, all are related to combustion phenomena. In this industrial and modern era of technology, the increasing demand for clean and efficient combustion is conditioned upon a good understanding of the underlying physics of combustion under turbulent conditions. With the advent of high performance computing, the scientific approaches toward combustion have significantly changed. Numerical methods and new approaches in turbulence are treated as cutting edge tools in simulation of the combustion process. Not to mention, the efficient, accurate, reliable and low cost simulations are yet a remarkable challenge for scientists and engineers. Several numerical approaches can be used to solve a combustion problem. In modeling turbulent combustion, three major approaches have been adopted: Reynolds-Averaged Navier-Stokes (RANS), Large-Eddy Simulation (LES), and Direct Numerical Simulation (DNS) [1]. In DNS, the Navier-Stokes equations are solved with full resolution to determine velocity field for one realization of the flow. Because all length-scales and timescales have to be resolved, DNS is computationally expensive [2]. In DNS, the accuracy

and results are considered as reliable as the experimental data; although the highest attainable Reynolds numbers in a DNS are too low to model practical turbulent combustion flows [3]. In this model, it can be shown that the computational cost is directly proportional to the grid size used and the rate of chemistry. Therefore, DNS is highly expensive. RANS solves for the mean values of the flow field. In other words, the instantaneous governing equations are being averaged and the non-linear terms are being modeled with closure terms. Due to the averaging of the governing equations, the resolution of the flow field is lower compared to DNS. Hence, it is more affordable in cost. LES captures the large-scale physics of the flow while the small-scale motions effects are modeled [2]. This methodology is based on the Kolmogorov theory that the large scale effects depends on the boundary and initial conditions; however, the fine effects have a universal behavior. Large eddies in LES are resolved on the coarse grids whereas smaller eddies contributions are modeled by using subgrid scale models. Mathematically speaking, LES equations are evaluated by imposing a filter onto the DNS equation. Since the filtering results in reduction of mesh size, LES is less expensive and more convenient than DNS [4]-[6].

Summary of Comparing the Methods

- 1.1. In RANS, all the scales from integral scales up to dissipation range needs to be modeled.
- 1.2. In LES, part of the inertial sub range and the beginning of the dissipation scales is modeled.
- 1.3. In DNS, no modeling needs to be done but it solves resolution for all the range, i.e., from the large scales completely through dissipation scales.

1.2. Motivation

In modeling turbulent combustion, LES may be used to predict the large scale and small-scale effects in the flow field with a reasonable cost while preserving a good accuracy. On a side note, LES can indeed handle many flows that RANS cannot. Combustion by its nature is complex due to heat release and species, transport in the process. Accordingly, in these types of flow, a higher order of accuracy is desired to capture the fast chemistry and high rate of chemical process. The One-Dimensional Turbulence (ODT) model as a stochastic modeling is designed to capture these small-scale effects. Hence, by introducing ODT along with the LES, higher resolution is achieved. The coupling of the aforementioned models has been done by Cao and Echehki [7]. Furthermore, the reduction of computations inspires the strategy of an ODT-based flame embedding for turbulent non-premixed combustion, an approach introduced and developed by Sedhai and Echehki [8]-[10]. The remaining challenge is to spatially filter the density obtained by 1D ODT domains and map them into the coarse LES grids.

1.3. Objective

The proposed study is focused on the spatial filtering of the density in the aforementioned approach in order to pass the high-fidelity density scalar to the lower resolutions LES solver. This filter enables the flame-embedding approach to provide the LES cells with the precise ODT density field. The mathematical development delves into the physics and analytical geometry of the problem. In each time step, the filtering is implemented and is passed to LES cells. Then, a bounded scalar for the density is derived to blend the density scalar from pure mixing solutions and ODT domains, which retain the smoothness and accuracy of density along the flame surface and oxidizer.

1.4. Chapters Outline

The following topics are divided into 6 chapters:

- Chapter 2: Review and Discussion of One Dimensional Turbulence
- Chapter 3: The Large Eddy Simulation and Fire Dynamics Simulator
- Chapter 4: Multi-scale Flame-Embedding LES-ODT Strategy
- Chapter 5: Case Study and Density Spatial Filtering
- Chapter 6: Conclusion and Future Work

CHAPTER 2

One-Dimensional Turbulence

In this chapter, the **One Dimensional Turbulence** (ODT) model is introduced. The approach and governing equations is reviewed briefly and at the end, the application of the method in flame-embedding model is discussed. Its objective is to model a strategy for coupling of turbulent transport, diffusion and reaction processes. This model can be applied to simple turbulent flows evolving temporally and spatially [6].

2.1. Introduction

ODT was initially introduced by Kerstein [11]. ODT simulates the mixing process along a hypothetical one-dimensional line in the flow field. In order to simulate the flow, ODT resolves the temporal and spatial scales on this line. The main feature of ODT is the stochastic approach used for modeling stirring or turbulent advection. The turbulence effect in the scalar field is simulated by a method called triplet maps along with Monte Carlo simulation. Stand-alone ODT is used for the flows that are homogeneous in at least one spatial direction. The remarkable characteristic of ODT model is that it resolves molecular transport without involving any extra approximation [12], [13].

In summary, one-dimensional domains in ODT consider [7]:

- Chemistry
- Stirring (advective) Events
- Molecular transport (diffusion)

2.2 Governing Equations

In this section the governing equations for ODT are briefly reviewed. The equations are relevant to the present Lagrangian formulation where ODT solutions are advected along the flame surface. Note that turbulent transport is modeled stochastically whereas reaction and diffusion processes are implemented deterministically. An in-depth discussion of formulation and model has been presented in [6] and [7].

In the present formulation, the LES-ODT solution involves the advection of numerous ODT domains or elements along the flame. The advection is based on the filtered velocity, while the effects of the fluctuating components of the velocity are implemented as part of the ODT elements' solution. The ODT domains are identified with their anchor points and their orientation, which is maintained normal to the flame. The anchor moves at the fluid filtered velocity, \bar{u} , such that the anchor's position can be updated using [6]:

$$\frac{dx}{dt} = \bar{u} \quad (2.1)$$

The followings are the governing equations formulated for the ODT domains in a Cartesian grid; η is the coordinate system component along ODT domain. Note that the density is variable in the ODT solution, which can be computed using the ideal gas equation and the solution for the temperature and the species mass fractions. Also the velocity field can be

written into two components; filtered (resolved) component, \tilde{u}_i , and residual component, u_i^* . The former component is being modeled in LES and it is related to the large-scale transport; whereas the latter component accounts for the simulation of ODT turbulent stirring events.

$$u_i = \tilde{u}_i + u_i^* \quad (2.2)$$

In summary the ODT governing equations for each one-dimensional element are:

- **Conservation of Momentum**

$$\frac{\mathfrak{D}u_i}{\mathfrak{D}t} = \frac{1}{\rho} \frac{\partial}{\partial \eta} \left(\mu \frac{\partial u_i}{\partial \eta} \right) + \Omega_{u_i} \quad (2.3)$$

- **Conservation of Energy**

$$\frac{\mathfrak{D}T}{\mathfrak{D}t} = \frac{1}{\rho c_p} \left[\frac{\partial}{\partial \eta} \left(k \frac{\partial T}{\partial \eta} \right) - \dot{\omega}_F q \right] + \Omega_T \quad (2.4)$$

- **Conservation of Species**

$$\frac{\mathfrak{D}Y_k}{\mathfrak{D}t} = \frac{1}{\rho} \left[\frac{\partial}{\partial \eta} \left(\rho D_k \frac{\partial Y_k}{\partial \eta} \right) + \dot{\omega}_k \right] + \Omega_k \quad (2.5)$$

Also the equation of state for ideal gas is as follow:

- **Ideal Gas Equation of State**

$$\rho = \frac{p}{RT} \quad (2.6)$$

Note that in the governing equations above, $\mathfrak{D}/\mathfrak{D}t$ denotes the material (also called substantial, total) derivative used for the Lagrangian framework. Also subscript F in (2.4) stands for fuel. Here ρ, k, μ, R and c_p respectively represent density, thermal conductivity, viscosity, specific gas constant, and thermal heat capacity. Besides, q, D_k and Y_k represent heat release per unit mass of fuel, mass diffusivity and species mass fraction.

Term $\dot{\omega}_k$ in equations (2.4) and (2.5) refers to the source term due to reaction and the stochastic process is shown with Ω_k . Note that η is the coordinate on the ODT elements normal to the flame surface. Mean advection terms are not appeared in the equations above yet they have a stretching role for the flame, which should be taken into consideration.

The turbulence process modeling in the governing equations (Ω_k) are modeled stochastically using the “*triplet maps*” method. Modeling of the stirring event in ODT starts with the appropriate selection of Eddy size, location, rate of distribution and probability computation and ends with the triplet map [16].

2.3 ODT Scalars Calculation

In the previous section, the one-dimensional-turbulence governing equations were discussed. This section is focused on computing the values for the scalars appeared in equations (2.3) through (2.6), which is in accordance to with Fire Dynamics Simulator open source code. The viscosity, material diffusivity and thermal conductivity are approximated from kinetic theory since the temperature dependence of each plays an important role in combustion. For the present study, the chemistry is a one-step reaction mechanism of propane and oxygen. Having said that, the reaction between the fuel (C_3H_8) and oxidizer (O_2) can be written as:



2.3.1 Density

The equation of state for ideal gas is written to compute the density for each species in the computational domain. The specific gas constant can be expressed in terms of universal gas constant, mass fraction and molecular weight of each species. Thus

$$\rho = \frac{p}{RT} \quad (2.8)$$

and

$$R = \mathcal{R}_u \sum_k \frac{Y_k}{W_k} \quad (2.9)$$

where \mathcal{R}_u is the universal gas constant, $\mathcal{R}_u = 8.31432 \times 10^3 \frac{\text{J}}{\text{kmol.K}}$, Y_k is the mass fraction and W_k is the molecular weight of the species. Note that in equation (2.8), pressure is constant throughout this case study and temperature and mass fraction are the resolved by One-Dimensional Turbulence governing equations.

2.3.2 Mass Diffusivity

Diffusion refers to the instantaneous mixing resulted from the existence of the species concentration gradient. It can be shown that the mass diffusivity (D_{AB}) of a binary system is a function of temperature, pressure and composition. For multicomponent gas mixtures, Chapman-Enskog Theory [14], the binary diffusion coefficient (m^2/s) can be written as:

$$D_{AB} = \frac{2.66 \times 10^{-7} \sqrt{T^3}}{\sigma_{AB}^2 \Omega_D \sqrt{W_{AB}}} \quad (2.10)$$

This equation states the dependence of the diffusion coefficient on the temperature and species. In the equation below:

- σ_{AB} : “Collision diameter”, a Lennard-Jones parameter ($^{\circ}A$)

$$\sigma_{AB} = \frac{\sigma_A + \sigma_B}{2} \quad (2.11)$$

- Ω_D : “Diffusion collision integral”, dimensionless; refer to [15] and [16].

$$\Omega_D = \frac{1.06036}{\tilde{T}^{0.1561}} + \frac{0.19300}{\exp(0.47635\tilde{T})} + \frac{1.03587}{\exp(1.52996\tilde{T})} + \frac{1.76474}{\exp(3.89411\tilde{T})} \quad (2.12)$$

and

$$\tilde{T} = \frac{\kappa_B T}{\varepsilon_{A,B}} \quad (2.13)$$

In the equation above, \tilde{T} is a dimensionless temperature which is represented in terms of absolute temperature T , Boltzmann’s constant ($\kappa_B = 1.381 \times 10^{-23} \text{ J/K}$) and a characteristic mixture energy parameter. This characteristic can be estimated in terms of the Lennard-Jones (12-6) potential characteristic energies for species A and B ($\varepsilon_{A,B}$):

$$\varepsilon_{A,B} = \sqrt{\varepsilon_A \varepsilon_B} \quad (2.14)$$

Values of ε_k for different species are provided in Poling et al. (2000) [16].

- W_{AB} can be obtained using:

$$W_{AB} = 2 \left(\frac{1}{W_A} + \frac{1}{W_B} \right)^{-1} \quad (2.15)$$

2.3.3 Gaseous Mixture Viscosity

The kinetic theory of Chapman and Enskog can also be applied for the viscosity of low-pressure multicomponent mixtures. The equations for viscosity of gas mixtures are generally

complicated. There are several interpolative methods: *Reichenberg, Wilke, Hering* and *Zipperer* are among these methods. In this study, the method suggested by Chung et al. is used to estimate the mixture viscosity. (Poling et al. [16]).

$$\mu_k = \frac{26.69 \times 10^{-7} (W_k T)^{1/2}}{\sigma_A^2 \Omega_\nu} \quad (2.16)$$

where σ_A is the Lennard-Jones hard-sphere diameter and is analogous to a molecular diameter, Ω_ν on the other hand is viscosity collision integral and it is obtained from the empirical equation below proposed by Neufeld et al.[15]:

$$\Omega_\nu = 1.16145(\tilde{T})^{-0.14874} + 0.52487e^{-0.77320\tilde{T}} + 2.16178e^{-2.43787\tilde{T}} \quad (2.17)$$

The gaseous mixture viscosity is given by:

$$\mu = \sum_k Y_k \mu_k \quad (2.18)$$

2.3.4 Specific Heat Capacity

The constant pressure specific heat of the mixture is obtained from:

$$c_p = \sum_k c_{p,k} Y_k \quad (2.19)$$

where $c_{p,k}$ is the temperature dependent specific heat of species k .

2.3.5 Thermal Conductivity

The thermal conductivity of species α is given by:

$$k_\alpha = \frac{\mu_\alpha c_{p,\alpha}}{Pr} \quad (2.20)$$

In calculating the thermal conductivity of the gas, Pr is the Prandtl number and it is assumed 0.7 for all cases [17].

On a side note, one assumption here is considering the nitrogen as dominant species in any combustion scenario and therefore the diffusion coefficient in the species mass conservation equation is that of the given species diffusion into nitrogen[17]:

$$(\rho D)_\alpha = \rho D_{\alpha, N_2} \quad (2.21)$$

2.3.6 Mass Production Rate

The chemical mass production rate of species α per unit volume for fuel (C_3H_8) and oxidizer (O_2) in equations (2.4), (2.5) are obtained from the equations (2.22),(2.23) below. As a convention, the subscript “ F ” is used for fuel and “ O ” to denote the oxidizer.

$$\dot{\omega}_F''' = -B(\chi_F \chi_O) e^{\left(\frac{E_a}{R_u T}\right)} \quad (2.22)$$

$$\dot{\omega}_O''' = 5 \dot{\omega}_F''' \frac{W_O}{W_F} \quad (2.23)$$

B , E_a , and χ_α represent the pre-exponential factor, activation energy and mole fraction of species' α respectively. Note that $B = 2.9 \times 10^{19} \frac{cm^3}{moles}$ and $E_a = 38.5 \frac{kCal}{mole}$ for the complete reaction of fuel and oxidizer (stoichiometric) [9][10][18].

CHAPTER 3

Large-Eddy Simulation and Fire Dynamics Simulator

3.1 Introduction

Large-Eddy Simulation is a powerful method amongst the turbulence numerical simulation methods. The LES technique is increasingly becoming major tool for modeling combustion. It aims at computing the large scale effects directly while the small scales are modeled. The former scales are influenced by geometry and responsible for turbulent transport of heat and momentum, whereas the latter scales are universal in the flow field. Note that small scales are not universal for chemistry. In LES the small effects are filtered out yet their influence on the large-scale motions is statistically introduced [22] and [24]. By filtering the governing equations, unclosed terms appear and need to be addressed. The unresolved turbulent fluxes can be modeled by providing closure terms. In this chapter, LES governing equations are presented. Filtering and closing strategies are briefly discussed. Some features of Fire Dynamics Simulator such as Combustion Model are reviewed.

3.2 Large-Eddy Simulation

This model has provided combustion modeling with numerous and promising advances in results. There are several properties of this model, which makes it stand out among other models such as:

- LES models the unsteady large scale mixing instead of averaging it.
- LES is capable of predicting the instabilities emerging from the coupling between hydrodynamic flow field and heat release.
- LES computes the large-scale effects explicitly, which mostly depend on the geometry. In contrast, the small scales events are universal properties and thus turbulence modeling of the smallest scale structures can make it efficient and justifiable for combustion flows.

3.2.1 Filtering

As noted earlier, the governing equations are spatially filtered either in the physical space or spectral space. The filtering in LES corresponds to applying a low-pass filter. The filtered operation is expressed as:

$$\bar{\Psi}(\mathbf{x}) = \int \Psi(\mathbf{x}^*)F(\mathbf{x} - \mathbf{x}^*) d\mathbf{x}^* \quad (3.1)$$

where F represents the LES filter.

All the filters are normalized, which implies:

$$\int \int \int F(\mathbf{x})d\mathbf{x} = 1 \quad (3.2)$$

A mass-weighted filter also can be defined as:

$$\bar{\rho} \tilde{\Psi}(\mathbf{x}) = \int \rho\Psi(\mathbf{x}^*)F(\mathbf{x} - \mathbf{x}^*)d\mathbf{x}^* \quad (3.3)$$

$$\tilde{\Psi}(\mathbf{x}) = \frac{\overline{\rho\Psi}}{\bar{\rho}} \quad (3.4)$$

The filter above is called, Favre filtering. Common filters are: the cut-off filter, the box filter, the Gaussian filter, and the Cauchy filter [24].

In turbulent flows, any instantaneous quantity (Ψ) might be decomposed into a filtered component ($\bar{\Psi}$) and a fluctuating component (Ψ').

$$\Psi = \bar{\Psi} + \Psi' \quad (3.5)$$

In order to make a distinction between different types of filtering, the Favre Average is denoted by “ \sim ” and filtered quantity are shown by “ $-$ ”.

In the next section, the LES governing equations are presented.

3.2.2 Governing Equations

By filtering the instantaneous governing equations for fluid flow, the LES equations are obtained:

- **Conservation of Mass**

$$\frac{\partial \bar{\rho}}{\partial t} + \frac{\partial \bar{\rho} \tilde{u}_i}{\partial x_i} = 0 \quad (3.6)$$

- **Conservation of Momentum**

$$\frac{\partial (\bar{\rho} \tilde{u}_i)}{\partial t} + \frac{\partial (\bar{\rho} \tilde{u}_j \tilde{u}_i)}{\partial x_j} = -\frac{\partial \bar{p}}{\partial x_i} + \frac{\partial}{\partial x_j} (\bar{\tau}_{ij} + \tau_{ij}^{SGS}) + \bar{\rho} f_{b,i} \quad (3.7)$$

- **Conservation of Mixture Fraction**

$$\frac{\partial \bar{\rho} \tilde{Z}}{\partial t} + \frac{\partial \bar{\rho} \tilde{Z} \tilde{u}_i}{\partial x_i} = \frac{\partial}{\partial x_i} \left(\bar{\rho} \frac{\mu_T}{Sc_T} \frac{\partial \tilde{Z}}{\partial x_i} \right) \quad (3.8)$$

- **Conservation of Energy**

$$\frac{\partial(\bar{\rho}\tilde{h}_t)}{\partial t} + \frac{\partial(\bar{\rho}\tilde{u}_j\tilde{h}_t)}{\partial x_j} = -\frac{\partial}{\partial x_j}[\bar{\rho}(u_j\tilde{h}_t - \tilde{u}_j\tilde{h}_t)] + \frac{\partial\bar{p}}{\partial t} - \frac{\partial\bar{q}_i''}{\partial x_j} + \bar{q}''' - \bar{q}_b''' + \bar{\varepsilon} \quad (3.9)$$

- **Ideal Gas Equation of State**

$$\bar{p} = \frac{\rho\mathcal{R}_u T}{\bar{W}} \quad (3.10)$$

In equation (3.8), Sc_T is the subgrid scale Schmidt number and ν_t is the subgrid scale viscosity computed from Smagorinsky model. Equations (3.7)-(3.9) contain unclosed (unresolved) terms such as:

- (3.7): unclosed Reynolds Stress τ_{ij}^{SGS} – subgrid scale turbulence model used as closure
- (3.9): unclosed enthalpy fluxes $\bar{\rho}(u_j\tilde{h}_t - \tilde{u}_j\tilde{h}_t)$ and average dissipative rate $\bar{\varepsilon}$

In equation (3.7), τ_{ij}^{SGS} represents the subgrid scale (SGS) stress and is expressed as equation (3.13) in the next section. Note that \bar{q}_i'' , \bar{q}''' and \bar{q}_b''' stated in (3.9) represent heat fluxes due to conduction and radiation, and heat release rate per unit volume, and heat transfer to evaporating droplets. Each can be computed as follows:

$$\bar{q}_i'' = -k \frac{\partial T}{\partial x_i} + \sum_{\alpha} h_{\alpha} \rho D_{\alpha} \frac{\partial Y_{\alpha}}{\partial x_i} + \bar{q}_{r,i}'' \quad (3.11)$$

$$\bar{q}''' = \bar{\omega}_F \Delta H_F \quad (3.12)$$

3.2.3 Closure

By filtering the governing equations, there are terms that remain unresolved and require closure to be modeled. Since combustion occurs at the unclosed scales of the computations, addressing closure plays important role in combustion models. The scope of closures is beyond the current study; nonetheless, the closure terms used in the approach are worth to present.

The subgrid stress can be expressed as:

$$\tau_{ij}^{SGS} = \bar{\rho}(\tilde{u}_i\tilde{u}_j - \widetilde{u_i u_j}) \quad (3.13)$$

Smagorinsky model, [25], offers a gradient-diffusion model to represent the subgrid transport. The eddy viscosity model provides a closure term for unresolved momentum flux [26]:

$$\tau_{ij} = \mu \left[\left(\frac{\partial u_i}{\partial x_j} + \frac{\partial u_j}{\partial x_i} \right) - \frac{2}{3} \delta_{ij} \frac{\partial u_k}{\partial x_k} \right] \quad (3.14)$$

The equation above can also be written in terms of subgrid scale viscosity (ν_t) and symmetric strain tensor (S_{ij}):

$$\tau_{ij} - \frac{\delta_{ij}}{3} \tau_{kk} = -2\nu_t S_{ij} \quad (3.15)$$

where symmetric strain tensor is defined as:

$$S_{ij} = \frac{1}{2} \left(\frac{\partial u_i}{\partial x_j} + \frac{\partial u_j}{\partial x_i} \right) \quad (3.16)$$

and δ_{ij} is the Kronecker delta.

The energy dissipation rate (ε) is given by:

$$\varepsilon = \tau_{ij} \frac{\partial u_i}{\partial x_j} \quad (3.17)$$

It is important to realize that LES models the dissipative processes due to viscosity, thermal conductivity and material diffusivity happens at scales smaller than those that are explicitly resolved on the numerical grid. In other word, viscosity, thermal conductivity and diffusivity cannot be expressed directly. In the Smagorinsky model, the viscosity can be modeled as:

$$\mu_{LES} = \rho (C_s \Delta)^2 \left(2\bar{S}_{ij} \cdot \bar{S}_{ij} - \frac{2}{3} \left(\frac{\partial \bar{u}_k}{\partial x_k} \right)^2 \right)^{\frac{1}{2}} \quad (3.18)$$

In this equation, Δ is a characteristic length corresponding to the filter size, and C_s is an empirical constant. Note the bar over the quantities above indicates that they are computed on a numerical grid. Thermal conductivity and diffusivity are given by:

$$k_{LES} = \frac{\mu_{LES} c_p}{Pr_t} \quad (3.19)$$

$$(\rho D)_{LES} = \frac{\mu_{LES}}{Sc_T} \quad (3.20)$$

3.3 Fire Dynamics Simulator

In this section, a description about the Fire Dynamics Simulator (FDS), is presented. FDS is an open-source code developed by National Institute of Standards and Technology (NIST) in collaboration with VTT Technical Research Center of Finland, the Society of Fire Protection Engineers (SFPE) and currently is maintained by the Building and Fire Research Laboratory (BFRL) of NIST. This open source code is written in FORTRAN 90 and is aimed at solving

practical fire problems and serving as a resource for combustion studies such as sprinkler, heat detector, flame spread and fire growth[17].

3.3.1 Features and Assumptions

The main features of the FDS code include: a hydrodynamic model, a combustion model and radiation transport. Here, only a brief description is provided. Details can be found in [17].

FDS computes the governing equations with rectilinear grids. In FDS, the hydrodynamic boundary conditions near the wall uses the empirical correlation based on Werner and Wengle model, ([27] and [28]), whereas the solid surfaces are set as thermal boundary conditions and the empirical correlations are applied for the heat and mass transfer to and from solid surfaces.

3.3.2 Hydrodynamic Model

FDS uses a low-Mach number formulation for the solution of the Navier-Stokes equations for low-speed and thermally driven flow. The equations are based on the LES approach. The numerical scheme is explicit and has second order accuracy temporally and spatially. As mentioned earlier, the Smagorinsky model uses a gradient-diffusion model to represent the subgrid transport.

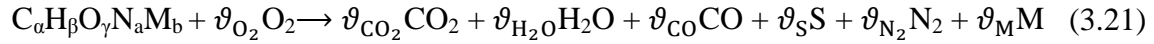
3.3.3 Radiation Transport

Radiation transport equation for a gray gas is used. A Finite Volume Method (FVM) is implemented to solve the radiation equation. The absorption and scattering coefficients in this scheme are according to Mie theory. This theory is expressed in [29] and provides the absorption and scattering coefficients in the scheme.

3.3.4 Combustion Model

The mixture fraction concept is implemented in FDS combustion model. The mixture fraction (Z) is defined as the ratio of mass of material having its origin in the fuel stream to the mass of mixture. The mass fraction (Y) can be obtained by the “State relations” from the mixture fractions (Figure 3.1). Note that mixture fraction is a conserved scalar. The mixture fraction-based combustion model is used for LES. This model is according to the Arrhenius reaction rate for each species, i.e. infinitely fast chemistry kinetics. The term “fast” implies that reactions occur so quick that there is no co-existence circumstance for fuel and oxidizer. The latter is presented in the following section.

The model used in the present study postulates a single-step, instantaneous reaction. This reaction of fuel and oxygen can be written as:



In the reaction above, S shows the soot which is a mixture of carbon and hydrogen, ϑ_S is the stoichiometric coefficient, M represents the additional products and $\alpha, \beta, \gamma, a, b$ are the number of the atoms in the fuel molecule. Hence, the mixture fraction can be expressed as:

$$Z = Y_F + \left(\frac{\vartheta_{CO}}{\alpha y_{CO}} \right) Y_{CO} + \left(\frac{W_F}{\alpha W_{CO_2}} \right) Y_{CO_2} + \left(\frac{\vartheta_S}{\alpha y_S} \right) Y_S \quad (3.22)$$

it yields:

$$Z = Y_F + \left(\frac{W_F}{\alpha W_{CO}} \right) Y_{CO} + \left(\frac{W_F}{\alpha W_{CO_2}} \right) Y_{CO_2} + \left(\frac{W_F}{\alpha W_S} \right) Y_S \quad (3.23)$$

Since the mixture fraction is a function of time and space, it is expressed as $Z(\mathbf{x}, t)$. The flame surface is where the oxidizer and fuel meet under stoichiometric conditions. The assumption of fast chemistry implies the fuel and oxidizer vanish at flame surface:

$$Z(\mathbf{x}, t) = Z_f = \frac{Y_{O_2}^\infty}{sY_F^I + Y_{O_2}^\infty} \quad (3.24)$$

in which:

$$s = \frac{\vartheta_{O_2} W_{O_2}}{\vartheta_F W_F} \quad (3.25)$$

In equations above, Z_f is the stoichiometric mixture fraction, $Y_{O_2}^\infty$ is mass fraction in oxidizer supply, Y_F^I is the mass fraction in fuel supply and $\vartheta_F = 1$.

The mixture fraction in equation (3.23) can be rewritten into two components Z_1 and Z_2 :

$$Z_1 = Y_F \quad (3.26)$$

$$Z_2 = \left(\frac{W_F}{\alpha W_{CO}} \right) Y_{CO} + \left(\frac{W_F}{\alpha W_{CO_2}} \right) Y_{CO_2} + \left(\frac{W_F}{\alpha W_S} \right) Y_S \quad (3.27)$$

$$Z = Z_1 + Z_2 \quad (3.28)$$

There are circumstances in which the fuel and the oxygen may mix but not burn. This intricate situation may be predicted based on the concentration and temperature of the gases adjacent to the flame surface. The partitioning of terms into two components helps to understand if the condition is met for the reaction to happen. Therefore, for describing the composition of the mixture at least two scalar variables are required. In the equation above, Z_1 shows the unburned fuel mass fraction and Z_2 is the burned fuel mass fraction.

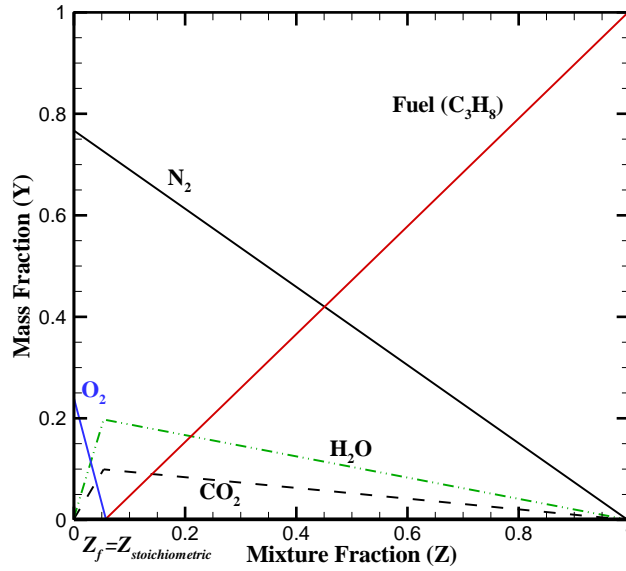


Figure 3.1 State relations for propane [30]

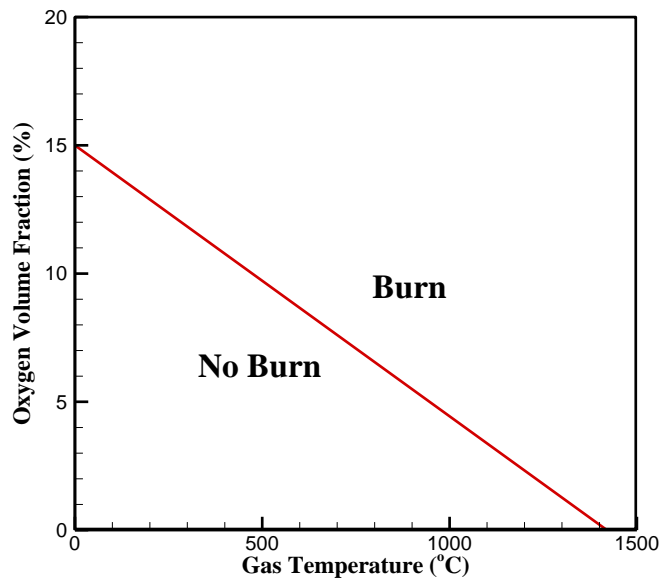


Figure 3.2 Oxygen-temperature phase space presenting where combustion is allowed or not allowed to take place[30]

Accordingly, the species mass fraction in the mixture can be found by:

$$Y_F = Y_F^I Z_1 \quad (3.29)$$

$$Y_{CO_2} = Y_F^I \frac{\vartheta_{CO_2} W_{CO_2}}{W_F} Z_2 \quad (3.30)$$

$$Y_{O_2} = Y_{O_2}^\infty (1 - Z) - Y_F^I \frac{\vartheta_{O_2} W_{O_2}}{W_F} Z_2 \quad (3.31)$$

$$Y_{N_2} = Y_{N_2}^\infty (1 - Z) + Y_{N_2}^I Z_1 + Y_F^I \frac{\vartheta_{N_2} W_{N_2}}{W_F} Z_2 \quad (3.32)$$

$$Y_{H_2O} = Y_F^I \frac{\vartheta_{H_2O} W_{H_2O}}{W_F} Z_2 \quad (3.33)$$

$$Y_{CO} = Y_F^I \frac{\vartheta_{CO} W_{CO}}{W_F} Z_2 \quad (3.34)$$

$$Y_S = Y_F^I \frac{\vartheta_S W_S}{W_F} Z_2 \quad (3.35)$$

$$Y_M = Y_F^I \frac{\vartheta_M W_M}{W_F} Z_2 \quad (3.36)$$

$$\vartheta_{CO_2} = \alpha - \vartheta_{CO} \quad (3.37)$$

$$\vartheta_{\text{H}_2\text{O}} = \frac{\beta}{2} \quad (3.38)$$

$$\vartheta_{\text{N}_2} = \frac{a}{2} \quad (3.39)$$

$$\vartheta_{\text{M}} = b \quad (3.40)$$

$$\vartheta_{\text{CO}} = \frac{W_{\text{F}}}{W_{\text{CO}}} y_{\text{CO}} \quad (3.41)$$

$$\vartheta_{\text{O}_2} = \frac{\vartheta_{\text{CO}} + \vartheta_{\text{H}_2\text{O}} - \gamma}{2} + \vartheta_{\text{CO}_2} \quad (3.42)$$

In equation (3.41), y_{CO} corresponds to the soot yield. Soot is postulated to be the mixture of the carbon and hydrogen.

CHAPTER 4

LES-ODT Model and Implementation

In this chapter, the model based on Large-Eddy Simulation and One-Dimensional Turbulence is reviewed. The coupling of the governing equations and passing data between the two solvers are discussed. Then, the implementation of the model in the proposed flame-embedding approach is presented.

4.1 LES-ODT Framework and Passing Information

In the present LES-ODT approach, the Lagrangian framework is selected for capturing the flame. In previous chapters, each of the solvers and their governing equations were discussed. In LES-ODT framework, the two models of LES and ODT are coupled. In the present study, the LES-ODT approach is used for the simulation of non-premixed flame where the flame surface is found by tracking the stoichiometric mixture fraction from LES; however, many features of the model formulation can be applied to other flames, premixed and non-premixed. The large-scale effects of the flow are captured by LES. The ODT elements are introduced and attached through their mid-point to the flame surface. These domains are oriented in the direction normal to the flame brush. The normal to the flame front is obtained by normalized gradient of mixture fraction corresponding to the stoichiometric condition. The next step is solving the governing equations on the one-dimensional domains. The ODT model is used to solve for momentum, energy and species

mass fractions. The ODT scalars such as density, mass diffusivity, gaseous mixture viscosity, thermal conductivity, etc. are calculated as described in the previous chapter. These properties are estimated based on the kinetic theory where properties are temperature dependent. The velocity and mixture fraction are interpolated from LES into ODT domains by tri-linear interpolation scheme (Appendix A). The LES velocity substitutes the large-scale component of the ODT velocity. The governing equations along the ODT domains are solved. The flame structure is resolved by ODT model.

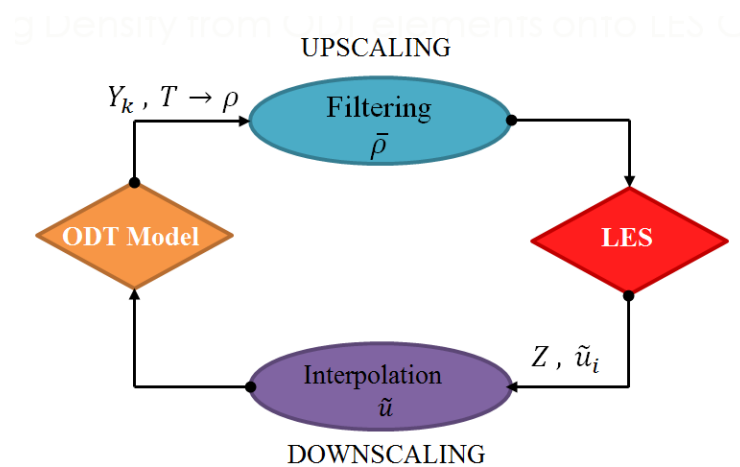


Figure 4.1 Coupling of LES with ODT and passing the information between two solvers

As shown in Figure 4.1 once the ODT equations are solved, the density can be obtained for grid points on the elements using the equation-of-state for the ideal gas. Since only ODT “sees” directly heat release, a filtered density is computed from ODT and passed to LES. This filtering corresponds to an upscaling process. The method of cubature is used for this purpose. Development of this spatial filter is addressed and discussed in next chapter. The coupling cycle of the LES with ODT is accomplished once the filtered density is passed to

LES. Modeling of the stirring event in ODT starts with the selection of eddy size and position and ends with the triplet map[11].

Note that ODT domains are advected through their anchor point. The anchor point velocity for each ODT domain can be calculated from LES velocity field as follows:

$$\tilde{u}_i = \frac{dx_i}{dt} \quad (4.1)$$

During the flame evolution, the clustering of the ODT elements is managed by removing the elements in dense area and introducing new domains at lower density regions and inlet [8].

CHAPTER 5

Density Filtering Procedure

This chapter is devoted to an approach developed to spatially filter the information from high-resolution one-dimensional-turbulence model grids, attached to flame brush, to the coarse grid of Large-Eddy-Simulation. In particular, the aim of density filtering presented here is to provide LES solver with the density attained from ODT solver by filtering it into LES cells. Although the primary focus of the approach is on filtering the density, this algorithm can be applied to the source terms as well. Moreover, the strategy is followed by smoothing step and blending the ODT solutions filtered into LES cells and the pure-mixing LES solution computed in Fire Dynamics Simulator right before passing the data to LES solver.

5.1 Overview

The previous chapters described the need for passing the filtered density to the LES solver right after the density is resolved by the one-dimensional turbulence model. At each LES time step, the density profile is computed on each grid point of the ODT domains, and a procedure for density filtering is implemented. The problem of density filtering has been addressed in [8],[9] by Sedhai and Echehki briefly and the feasibility of the Radial Based Function (RBF) method as a method for density filtering have been presented by these authors. It was noted that this method is not a possible solving strategy for flame-embedding

approach; nevertheless it can be a case study for further investigation by introducing the proper modifications. In the current study, an algorithm is developed and implemented in order to pass the density to the LES solver. The spatial filter scheme exploits the Gaussian Cubature Method. Additionally, the implemented method is optimized to perform the task without any further cost of computation. Finally, a density blending scheme is introduced to obtain a smooth density throughout the entire domain by combining density from ODT with density from the FDS solution of pure mixing outside the flame. In the following sections, the steps above are discussed in details and the case study and simulation results are presented in Chapter 6.

5.2 Spatial Filtering (Upscaling)

As mentioned earlier in this chapter, the spatial filtering process is not limited to the filtering of the density but also molecular flux and source terms in the flame-embedding approach. However, it is implemented here only for density filtering. First, the filtering must account for the fact that 1-D ODT domains are attached normal to the flame surface. At each simulation time step, the density for the ODT domains is evaluated using the ODT model discussed in the previous chapters. Each ODT domain contains a number of grid points, which define the fidelity of the small scale domain. As a convention, the subscript “*LES*” and “*ODT*” are used to describe the coordinates and positions of each grid system. As shown in Figure 5.1 below, a schematic of the flame-embedding strategy and its description, which leads to a spatial filtering approach, are illustrated for clarifying the problem.

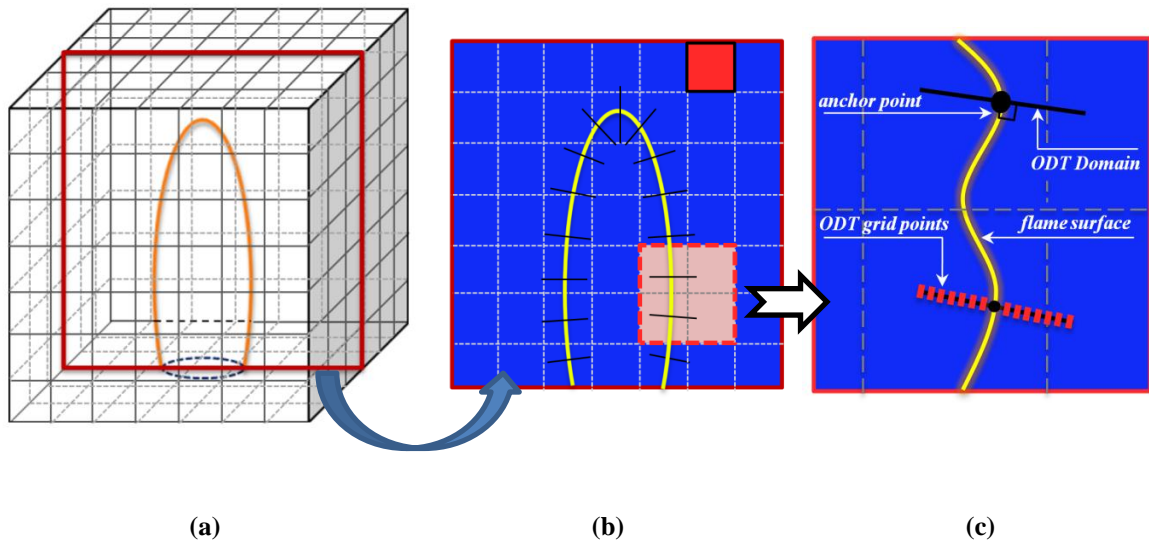


Figure 5.1 A schematic illustration of LES-ODT computational grid. Subfigure (a) presents the 3D flame brush and coarse grid of LES. Subfigure (b) shows a 2D cross section of the domain. Subfigure (c) illustrates a closer look at high resolution ODT domain attached to flame brush.

The leftmost Figure (a) shows the flame brush at a specific simulation time as delineated by the stoichiometric value of the filtered mixture fraction. Each ODT grid point on the one-dimensional elements is carrying evaluated information such as density ρ_{ODT} . Each ODT domain can be represented by its end-points. Similarly every point on the ODT domain can be specified by its position in the Cartesian coordinate system. The number of ODT points on each element determines the resolution of the subgrid solver. As described earlier, the surface of the flame can be computed by the mixture fraction Z corresponding to the stoichiometric condition. The solution for the mixture fraction is carried out in LES solver. All the embedded elements are oriented in the direction normal to the flame brush and fixed via the anchor point. In Figure (b) the ODT elements are shown. Due to the higher resolution of the ODT grids, every LES cell adjacent to the elements includes lines of ODT

points. Thus, the effect of each ODT grid point has to be taken into account and this contribution should be modeled. In particular, this contribution is not only due to the number of the ODT points present within a LES cell but also should be a function of their distance to LES cell center. The proposed spatial filtering method uses a distance-based weighting function called the cubature method. Furthermore, several tasks and corresponding algorithm are developed to reduce the cost of the computation. These tasks include pre-filtering the density on each ODT domain, applying the Gaussian as the kernel function for the cubature method, introducing cut-off for the Gaussian function, and eventually investigation and using a function for blending and smoothing the density attained from ODT and FDS.

In the subsequent sections below, the developed scheme is discussed in detail. The scheme is validated by simple test cases. Eventually, the approach is implemented in the LES-ODT flame-embedding approach and the density field is passed to LES as discussed earlier.

5.2.1 The Gaussian Cubature Method

A principal implementation of the spatial filter relies on the method of cubature. Each LES cell is allotted a contribution from ODT grid point in its vicinity. As stated in the previous section, this contribution is related to the distance of the LES cell center and the ODT grid point (\mathbf{r}). This distance can be found from relations (B.7) to (B.10) in Appendix B.

The cubature method consists of finding an approximate calculation of a triple integral on a domain Δ and it is given by:

$$\int_{\Delta} \varphi(\zeta) d\zeta = \bar{\varphi} \int_{\Delta} d\zeta \quad (5.1)$$

Note the weighting of each ODT grid point on the adjacent LES cells decays as a function of its distance from any LES grid center. A Gaussian weighting function is introduced as the kernel function in cubature method in the above equation. The integrand and general equation for the Cubature Method for the scalar ρ (density here) can be written as:

$$\varphi(\zeta_k) = \rho_k \omega(\zeta_k) \quad (5.2)$$

$$\int_{\Delta} \rho_k \omega(\zeta_k) d\zeta = \bar{\rho} \int_{\Delta} \omega(\zeta_k) d\zeta \quad (5.3)$$

In equation above, the kernel function $\omega(\zeta_k)$ is the Gaussian weighting function and the left hand side is called Gaussian Weighted Integral (known as Gaussian Cubature Method) [19]. Since the domain is discretized, the summation is substituted over the computational domain.

$$\sum_k \rho_k \omega(\zeta_k) = \bar{\rho} \sum_k \omega(\zeta_k) \quad (5.4)$$

This procedure is applied in order to spatially filter the density (it can be another source term also) onto the LES cells. The equation (5.4) above can be rewritten as:

$$\bar{\rho}_{LES} = \left(\sum_k \rho_k \omega(\mathbf{r}^*) \right) / \left(\sum_k \omega(\mathbf{r}^*) \right) \quad (5.5)$$

In equation (5.5), \mathbf{r}^* is defined as the dimensionless distance from LES center node to an ODT element, $\omega(\mathbf{r}^*)$ is the Gaussian weighting function, ρ_k is the density of the tagged

ODT point, and $\bar{\rho}_{LES}$ is the filtered density onto LES cell center. Thus, the process has an upscaling behavior.

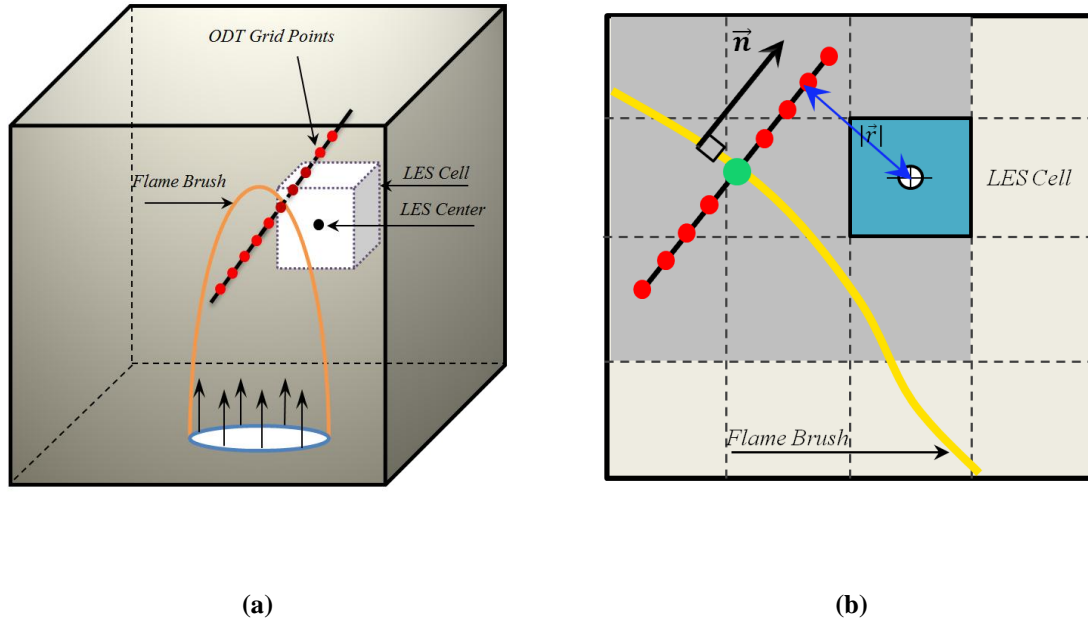


Figure 5.2 (a) The LES cell and ODT Element attached to the flame surface in 3D
 (b) The relative positions of the ODT Grid Point and LES cell in influenced region

This is demonstrated in Figure 5.2. Every LES cell in the influenced region around the ODT domain is captured as discussed in next section below and the corresponding weighting factor, $w(\mathbf{r}^*)$, and weighted density, $\rho_k w(\mathbf{r}^*)$, are tagged within each cell.

5.2.2 Influence Domain and Effective Radius

The proposed spatial filtering exploits a region of influence around each high resolution ODT element. The LES cells that are distant from the ODT elements have a negligible contribution from ODT grid points. Therefore, LES grids are simply discarded by a cut-off

Gaussian kernel function in filtering process; therefore, the cost of computation is significantly decreased. The criteria defined for the influenced domain would be restricted to a dimensionless radius called an effective radius. The locus of all LES center points located in a specific distance from ODT element implies a cylindrical effective region of influence around each ODT elements. Therefore, a cylindrical coordinate system is chosen so that its axis is oriented in the normal direction to the flame surface (shown in Figure 5.3). Note that the effective radius is of the order of the ODT element length and defined by:

$$r^* = \frac{r}{\mathcal{R}_{eff}} \quad (5.6)$$

The two hemispheric regions attached to the cylinder, shown in Figure (a), account for the ending effects of each one-dimensional turbulence domains. Figure (b) exhibits the ODT

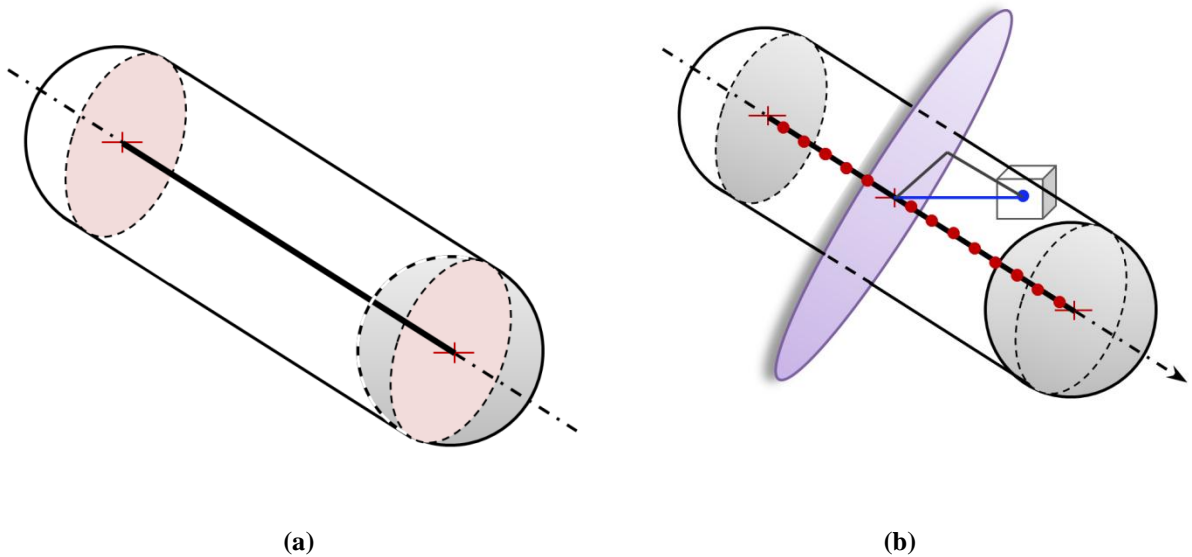


Figure 5.3 (a) Effective domain adopted for filtering
(b) Effective domain oriented in the direction normal to the flame surface

domain enclosed by the region of influence and cylindrical coordinate system used for filtering. Having said that, the Cut-Off Gaussian as a kernel function is formulated as below:

$$w(r^*) = \exp\left(-\frac{r^{*2}}{\sigma^2}\right) \quad (5.7)$$

In the equation (5.7), σ defines a secondary scaling factor by which the rate of decaying Gaussian kernel function is controlled. This factor is equivalent of having more ODT domains involved in filtering procedure and defines an effective bandwidth for filtering.

5.2.3 Blending of the Filtered Density Solutions

In the previous section, the scheme for upscaling the density from One-Dimensional Turbulence model into LES grid was discussed. Since the ODT elements are placed near the flame and the filtering may not implemented away from the flame, blending of the LES filtered density solution with a non-reacting density solution from LES is needed to cover the entire LES computational domain. The filtered density (ρ_{ODT}^{LES}) is mapped onto the density obtained by pure mixing solution (ρ_{FDS}^{LES}). A blending method is implemented in order to blend the solution at the overlapped region (Figure 5.4). This is done by introducing an average cell properties based on a blending function, α .

$$\rho_{ave} = \alpha\rho_{ODT}^{LES} + (1 - \alpha)\rho_{FDS}^{LES} \quad (5.8)$$

Note that filtered density obtained by ODT provides density solely for LES grids within the flame embedded region.

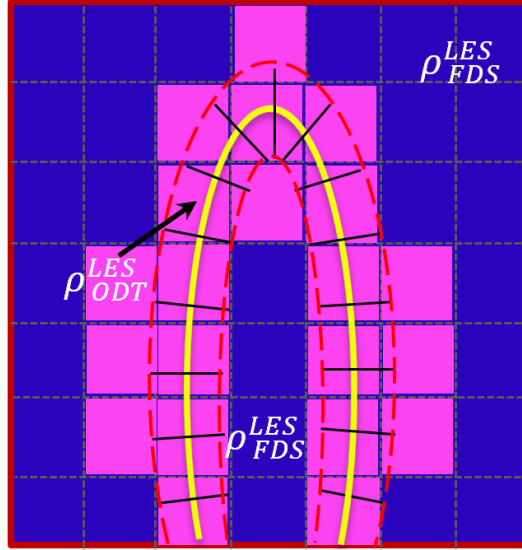


Figure 5.4 Blending pure mixing solution and filtered density based on ODT solution

The blending function α is a non-dimensional parameter that is interpreted as a measure of confidence in the availability of adequate ODT data to determine the ODT-based filtered density. Therefore, it is evaluated based on the accumulated weighting, $\sum w(\mathbf{r}^*)$, of filtered density in each LES cell:

$$\kappa_{i,j,k} = \sum w(\mathbf{r}^*) \Big|_{i,j,k} \quad (5.9)$$

$$\kappa_{max} = \max(\kappa_{i,j,k}) \quad (5.10)$$

$$\varepsilon_{i,j,k} = \frac{\kappa_{i,j,k}}{\kappa_{max}} \quad (5.11)$$

$\varepsilon_{i,j,k}$ is evaluated at each upscaled LES cell. According to this value and a smoothing function below, α is determined. $\alpha_{i,j,k}$ is indeed a measure for contribution of spatially filtered density and FDS density; $\alpha_{i,j,k}$ close to 1 indicates that there is a significant contribution of ODT points in the cell, and thus, it has to have a higher contribution to LES solution than FDS solution in that particular cell.

A bounded smoothing function below is postulated in a general form of:

$$\alpha_{i,j,k} = \frac{1}{2}(1 + \tanh(c_1(\varepsilon_{i,j,k} + c_2))) \quad (5.12)$$

The function has a domain and range in $[0,1]$ interval whereas constants c_1 and c_2 are responsible for the stretching/compressing and sliding of the smoothing function.

Figure 5.5 below shows the smoothing function and its trend for different values of constants c_1 and c_2 . Note that the domain and smoothing function range lies between zero and unity.

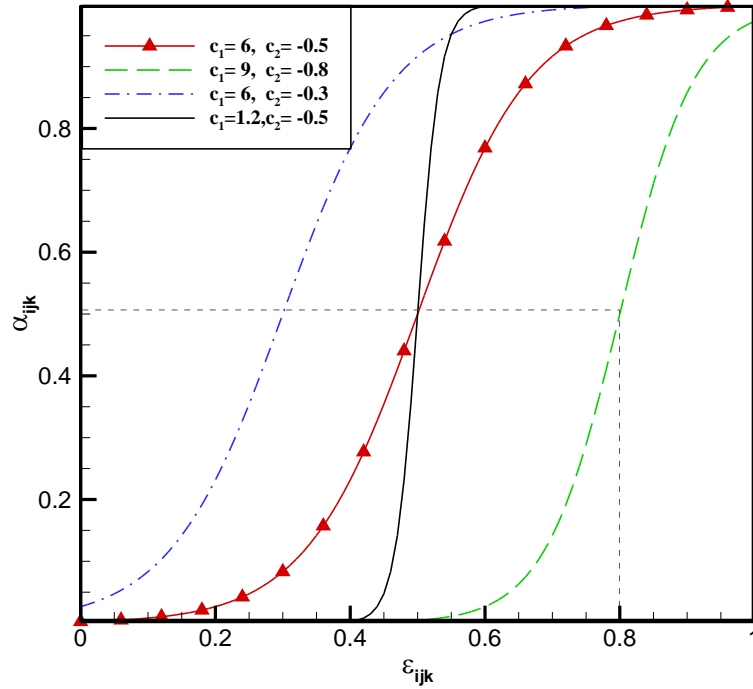


Figure 5.5 Smoothing function used for blending the density from LES-ODT and FDS solution

$$\alpha_{i,j,k} = \frac{1}{2} (1 + \tanh(c_1(\epsilon_{i,j,k} + c_2)))$$

Hence, an array of $\alpha_{i,j,k}$ are computed during the spatial filtering of the density and is evaluated by equation (5.12) in transition from attained ODT solution adjacent to the flame surface to the FDS solution around.

The Figure 5.6 illustrates the flow chart for the filtering process.

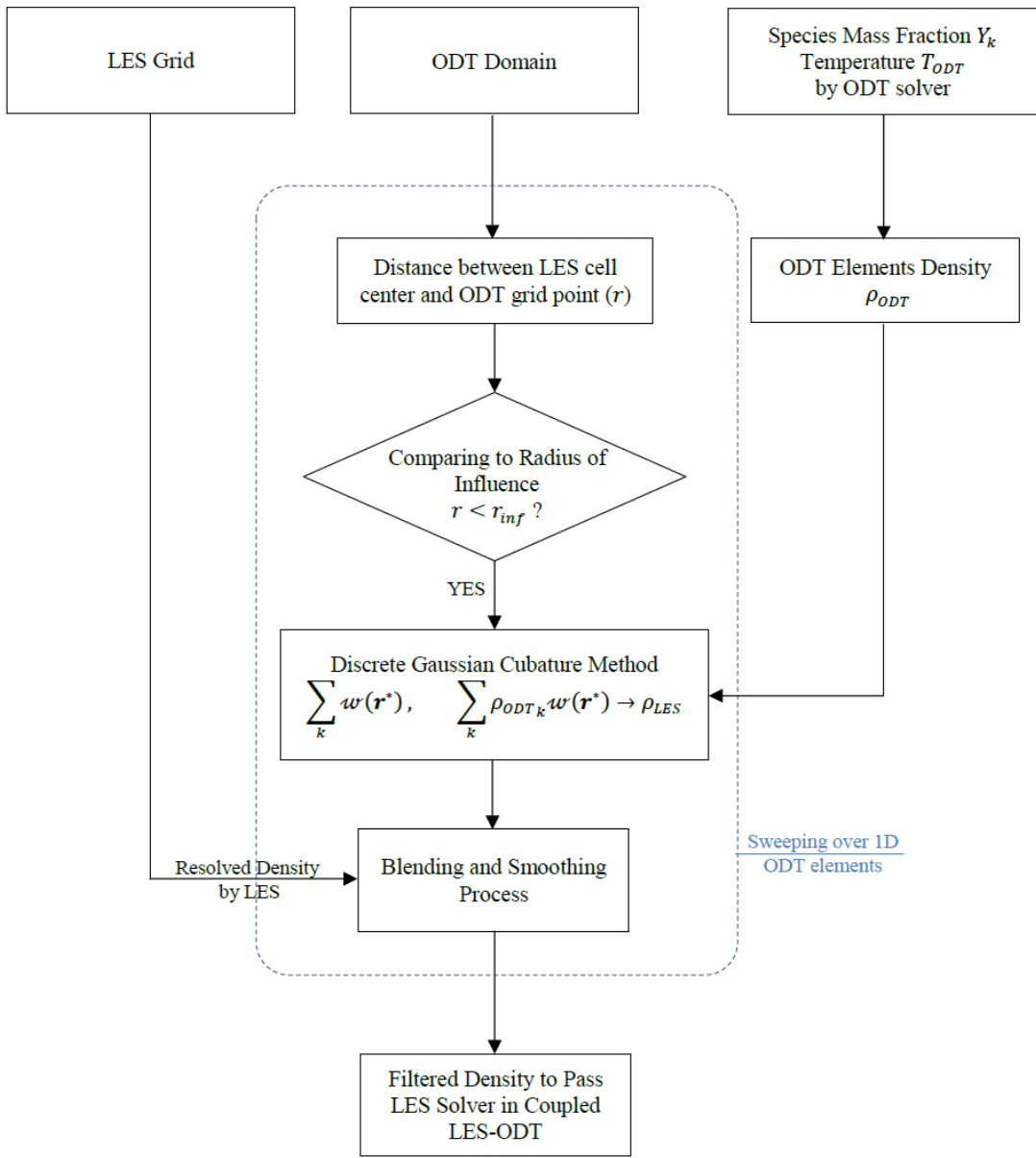


Figure 5.6 Flow chart of proposed spatially filtering density for LES-ODT

CHAPTER 6

LES-ODT Simulation: Non-Premixed Propane - Air Jet Flame

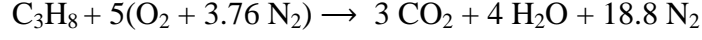
6.1 Objectives

In this chapter, the LES-ODT flame-embedding approach is used to simulate a turbulent non-premixed propane-air jet flame. First, the simulation conditions are presented. Then, the governing equations specific to the problem is reviewed. The implementation of the developed algorithm and strategy is discussed. The filtered density field is presented at 3 different simulation time. The trend of scalars such as density, temperature, fuel mass fraction and oxidizer mass fraction along an ODT domain are exhibited. The effect of finite chemistry on temperature is presented.

6.2 Simulation Conditions

To validate the flame-embedding modeling approach, a simulation of a turbulent non-premixed flame of propane-air is performed. This simulation is governed by the coupled LES-ODT model using a Lagrangian framework. Here, the governing equations are reviewed concisely. Simulation conditions including boundary conditions, geometry of the problem, resolution of the grids and finally the ODT domains characteristics are explained.

The simulation of non-premixed propane-air flame jet uses a one-step reaction mechanism of propane (C₃H₈) and (O₂) oxygen as follows:



6.2.1 Governing Equations for LES-ODT Flame-Embedding Approach

LES Governing Equations:

- *Conservation of Mass*

$$\frac{\partial \bar{\rho}}{\partial t} + \frac{\partial \bar{\rho} \tilde{u}_i}{\partial x_i} = 0 \quad (6.1)$$

- *Conservation of Momentum*

$$\frac{\partial (\bar{\rho} \tilde{u}_i)}{\partial t} + \frac{\partial (\bar{\rho} \tilde{u}_j \tilde{u}_i)}{\partial x_j} = - \frac{\partial \bar{p}}{\partial x_i} + \frac{\partial}{\partial x_j} (\bar{\tau}_{ij} + \tau_{ij}^{SGS}) + \bar{\rho} f_{b,i} \quad (6.2)$$

- *Conservation of Mixture Fraction*

$$\frac{\partial \bar{\rho} \tilde{Z}}{\partial t} + \frac{\partial \bar{\rho} \tilde{Z} \tilde{u}_i}{\partial x_i} = \frac{\partial}{\partial x_i} \left(\bar{\rho} \frac{\mu_T}{Sc_T} \frac{\partial \tilde{Z}}{\partial x_i} \right) \quad (6.3)$$

ODT Governing Equations:

- *Conservation of Momentum*

$$\frac{\mathfrak{D} u_i}{\mathfrak{D} t} = \frac{1}{\rho} \frac{\partial}{\partial \eta} \left(\mu \frac{\partial u_i}{\partial \eta} \right) + \Omega_{u_i} \quad (6.4)$$

- *Conservation of Energy*

$$\frac{\mathfrak{D}T}{\mathfrak{D}t} = \frac{1}{\rho c_p} \left[\frac{\partial}{\partial \eta} \left(k \frac{\partial T}{\partial \eta} \right) - \dot{\omega}_F q \right] + \Omega_T \quad (6.5)$$

- *Conservation of Species for Oxidizer*

$$\frac{\mathfrak{D}Y_{\mathbf{O}}}{\mathfrak{D}t} = \frac{1}{\rho} \left[\frac{\partial}{\partial \eta} \left(\rho D_{\mathbf{O}} \frac{\partial Y_{\mathbf{O}}}{\partial \eta} \right) + \dot{\omega}_{\mathbf{O}} \right] + \Omega_{\mathbf{O}} \quad (6.6)$$

- *Conservation of Species for Fuel*

$$\frac{\mathfrak{D}Y_{\mathbf{F}}}{\mathfrak{D}t} = \frac{1}{\rho} \left[\frac{\partial}{\partial \eta} \left(\rho D_{\mathbf{F}} \frac{\partial Y_{\mathbf{F}}}{\partial \eta} \right) + \dot{\omega}_{\mathbf{F}} \right] + \Omega_{\mathbf{F}} \quad (6.7)$$

- *Ideal Gas Equation of State*

$$\rho = \frac{p}{RT} \quad (6.8)$$

Note that in the equations above, the spatially filtered density solved by the ODT governing equations is passed to the LES equations.

6.2.2 Boundary Conditions and Geometry

The computational domain for the current simulation and the run conditions are presented in table 6.1 below. As it is illustrated in Figure 6.1, the domain is open to atmospheric pressure and has an inlet at the bottom. In the inlet, propane jet is injected with a co-flow of air at different velocities as described.

Table 6.1 Simulation Conditions for Non-premixed Turbulent Flame

Simulation Condition					
Description		parameter		Value	
Geometry	Computational Domain	Width		w_1	0.1 m
		Length		w_2	0.1 m
		Height		H	0.2 m
	ODT Grid	Element Length		L_{ODT}	16 mm
		Number of Grid Points		N_{ODT}	41
		Grid size		Δ_{ODT}	0.40 mm
	LES Grid	Grid size		Δ_{LES}	1.25 mm
		Number of Grids	x-direction	$N_{LES,x}$	80
			y-direction	$N_{LES,y}$	80
z-direction			$N_{LES,z}$	160	
Boundary Condition	Inlet	Geometry	Diameter	d	10 mm
		Velocity	Fuel	V_F	1 m/s
			Air	V_{Air}	0.5 m/s
		Properties	Pressure	p	1 atm
Temperature	T		300 K		
Chemistry	Fuel	Propane C_3H_8	Molecular Weight	W_F	44.1 g/mole
	Oxidizer	Air $O_2 + 3.76N_2$		W_O	28.966 g/mole

In Figure 6.1 the computational domain is shown. A structured Cartesian LES grid topology is used. The number of grid points on each ODT domain defines its resolution. Similarly,

the grid size for LES domain specifies the resolution of the coarse grid used for Large Eddy Simulation.

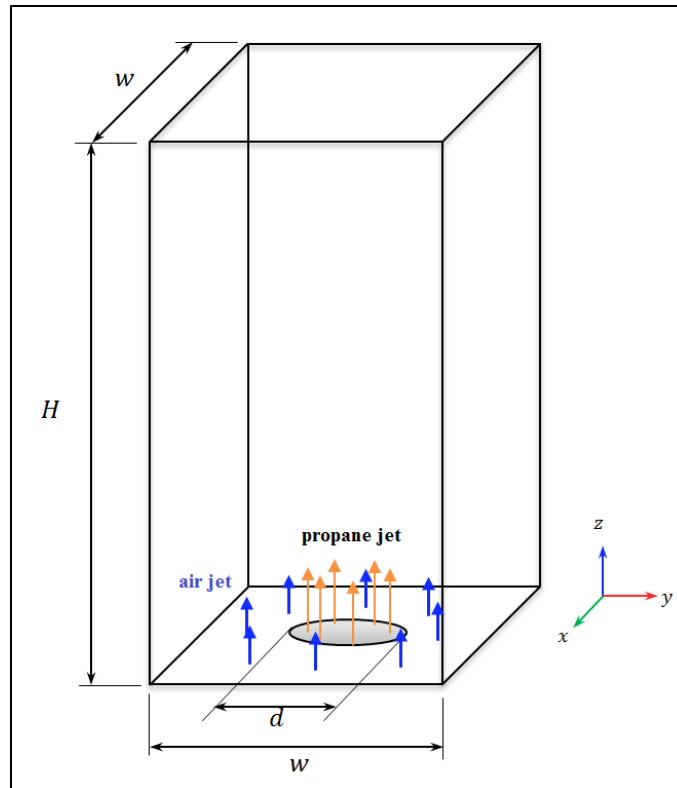


Figure 6.1 A schematic of the computational domain

6.2.3 Model Implementation

The implementation of the flame-embedding approach is initiated with standard solution in FDS based on the existing models for combustion in FDS. The FDS-based LES is designed to reach near statistically steady flow conditions before ODT elements are introduced for the more computationally demanding portion of the simulation. Since in the initial time steps the

flame is not fully developed, introducing the ODT elements is postponed until the flame has evolved. Afterwards, the ODT elements are attached to the flame brush at their anchor points. The flame surface is defined by the stoichiometric mixture fraction computed in FDS. This step is accompanied by the coupling and exchange of information between LES and ODT model. The ODT governing equations require the downscaled velocity and mixture fraction from LES. The downscaling process is performed by tri-linear interpolations from the LES grids to the ODT grids. This method estimates the value of an intermediate point within a cubical element (see Appendix B, [8], [9]). The anchor points are moved and developed as the flame is tracked. As the simulation time elapses, the number of ODT domains and their orientation will change.

Stirring events are implemented by performing triplet maps. Once the ODT governing equations are solved at a LES time step, the density is filtered to LES grids. The filtering process at each time step, as described in the previous chapter, consists of several stages.

These stages are:

1. The calculation of the temperature and mass fraction from mixture fraction provided by the LES solution
2. The calculation of the density at each ODT grid point
3. The tagging of the LES cells influenced by ODT domain
4. Book-keeping the distance of each LES cell and ODT elements
5. The recording of the coordinate of the projected LES cell on ODT element
6. Accessing the corresponding density of ODT grid point based on the projection point
7. The Application of the Gaussian Cubature Method

8. The calculation of filtered density
9. The smoothing of the solution by finding the contribution of the filtered density for LES cells and the FDS density
10. Finally, the density is passed to the LES solver and the coupling cycle continues

In the next section, the results are presented for different simulation times.

6.3 Results

In this section, the results of the LES-ODT simulation of a turbulent non-premixed propane-air jet flame are presented. The evolution of the flame is shown at different time steps. The arrangement of the ODT domains attached to the surface is presented. The fuel mass fraction, oxidizer mass fraction, temperature and density over an ODT domain are shown. The tagged LES cells captured in density filtering are shown. Finally, the smooth filtered density is exhibited.

The surface of the flame corresponds to the mixture fraction in stoichiometric condition, which is for propane and air is $Z_f = 0.059$. Each ODT element is oriented in the direction normal to the flame surface. This normal unit vector is given by:

$$\vec{n} = \frac{\nabla Z}{|\nabla Z|} \quad (6.9)$$

In Figure 6.2 and Figure 6.3, the ODT domains are shown. These elements adjust and evolve as the flame is developing. The cross-section of the flame is also illustrated to show how these ODT domains are attached and oriented. The ODT domains are uniformly located. The following is for the simulation time 0.19 s and 20 s. (Figure 6.2). As previously discussed, in spatial filtering, the weighted values for each cell are computed and normalized by the maximum of the accumulated weights. This parameter is referred to as the normalized cumulative weight factor (NCWF) and shown by $\varepsilon_{i,j,k}$. This latter parameter is defined to calculate the contribution of an ODT domain to the weights of an LES cell. Hence, a cell with a higher value of $\varepsilon_{i,j,k}$ indicates that more ODT elements have contribution and are dense in that region.

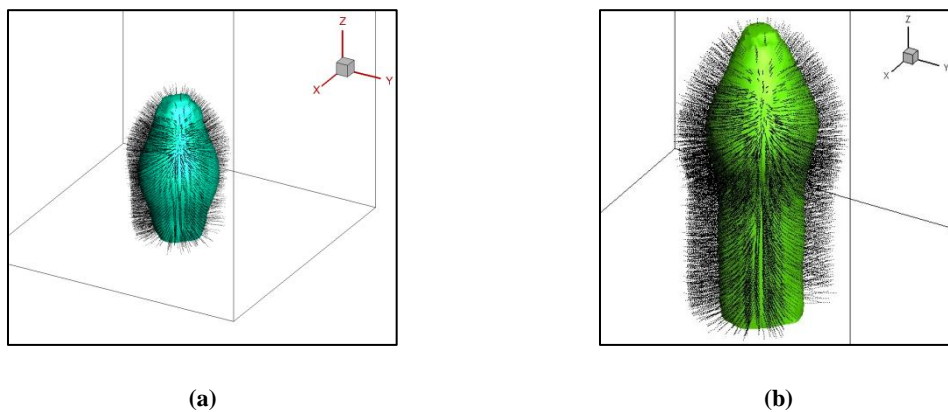


Figure 6.2 (a) Growth of flame brush and ODT elements attached at simulation time: 0.18s
 (b) Growth of flame brush and ODT elements attached at simulation time: 0.20s

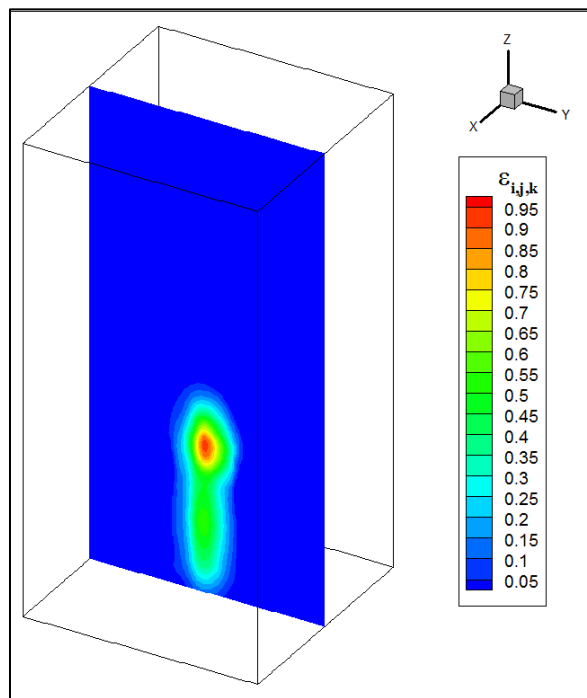


Figure 6.3 Contribution of the ODT domains to each LES cell in filtering process

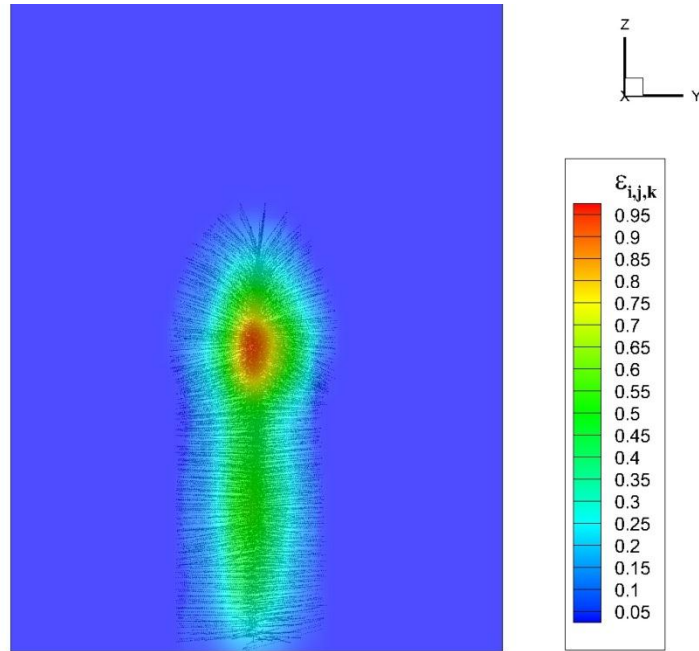


Figure 6.4 Overlapping ODT elements on NCWF contour ($\epsilon_{i,j,k}$)

As it is shown in the Figure 6.4, inside the flame the ODT domains are denser. The contribution of the ODT elements is noticeable. Outside of the flame this trend is opposite. In this region ODT domains are located more distant from each other and there is lack of data in those regions, which implies the FDS solution is the sole contributor to the coarse grids. In Figures 6.5 and 6.6, the temperature field computed from spatial-filtering is shown at two different solution times. This temperature field is obtained based on the ODT solution. Note that the embedding region is bounded by the end points of ODT elements.

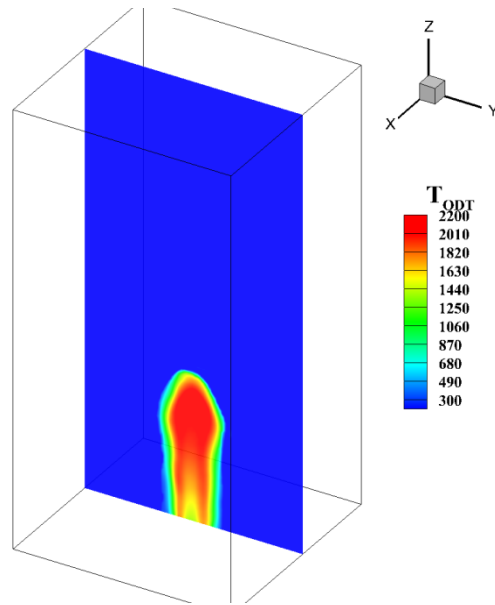


Figure 6.5 Temperature field at solution step 590

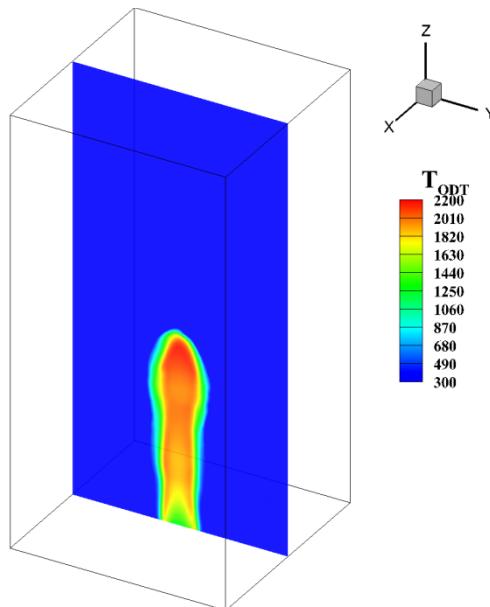


Figure 6.6 Temperature field at solution step 650

In Figures 6.7 and 6.8, the FDS density and spatially filtered density are shown. Note that the solution obtained from the filtered density has filtered some of the peaks as expected since filtering is a volume averaging process. Given the inverse relation between temperature and density in the ideal gas equation, the higher temperature corresponds to a lower density and *vice versa*. Thus, as it can be seen the peaks are filtered out in the spatially filtered density field.

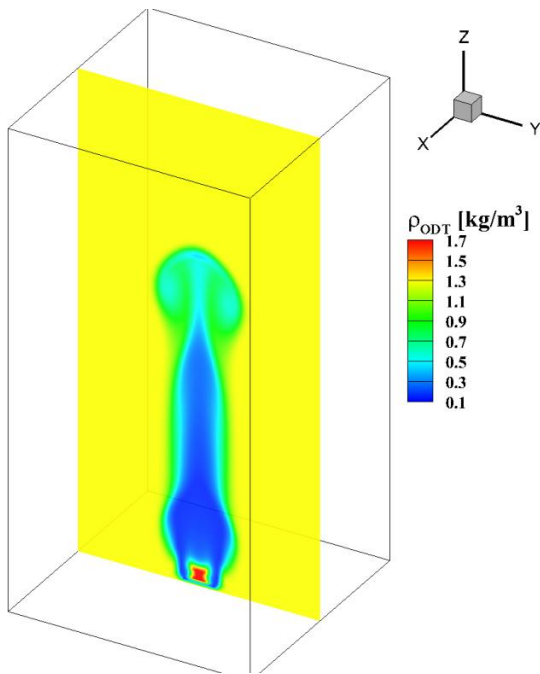


Figure 6.7 FDS Density

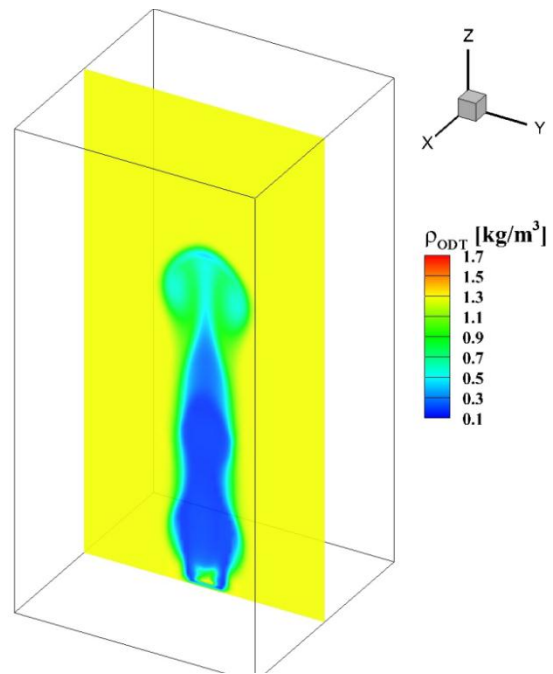


Figure 6.8 Filtered Density

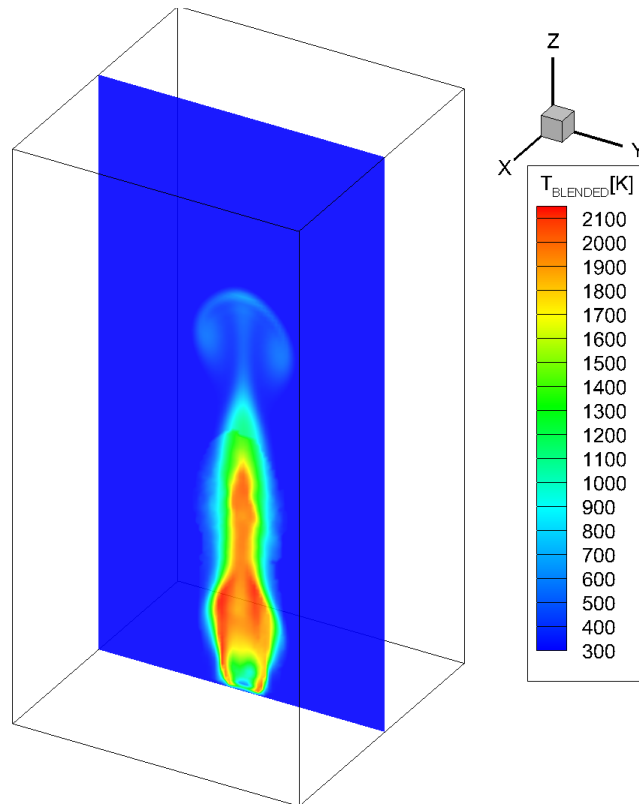


Figure 6.9 Temperature field at 22s

CHAPTER 7

Conclusion and Future Work

7.1 Conclusion

In this study, an approach for spatially filtering the density for flame-embedding using LES-ODT is developed. The Lagrangian embedding strategy is used for the simulation of a non-premixed flame. The LES model and ODT model are coupled in this framework. The small-scale effects are captured using the ODT high-resolution domains. The coupling and passing of the information between the two models is demonstrated. The upscaling of the density from ODT to LES is investigated and an algorithm is developed. The simple one-step air-propane reaction is modeled as a case study. The proposed filtering scheme for density completes the coupling step of LES-ODT approach for flame-embedding strategy.

7.2 Future Work

The current spatial filtering of the density used the Gaussian Cubature Method for upscaling the density of ODT elements onto the coarse grids of LES. Different approaches for spatial filtering can be adopted as well based on the kernel functions in the proposed approach. A scheme can be developed to optimize and control the density of ODT domains on flame surface locally and in particular flame tip where ODT elements are less dense. The validation of the numerical data with experimental data can be done.

REFERENCES

- [1] Kuo, Kenneth K., Yun Acharya, R., "*Fundamentals of Turbulent and Multi-Phase Combustion*", Wiley, 2012
- [2] Pope, Stephen B., "*Turbulent Flows*", Cambridge University Press, 2000
- [3] Beysiere, V., Jarosinski, J., "*Combustion Phenomena*", CRC Press, 2009
- [4] Peters, N., "*Turbulent Combustion*", Cambridge University Press, 2000
- [5] Poinso, T, Veynante, D., "*Theoretical and Numerical Combustion*", 2nd Edition, R. T. Edwards(Ed.), 2005
- [6] Echehki, T., "*Turbulent Combustion Modeling: Advances, New Trends and Perspectives*", Springer, 2011
- [7] Cao, S., Echehki, T., "*A Low-Dimensional Stochastic Closure Model for Combustion Large-Eddy Simulation*", Journal of Turbulence, 58(24): 1-35, 2008
- [8] Sedhai, S., Echehki, T., "*An ODT-Based Flame-Embedding Approach for Turbulent Non-Premixed Combustion*", AIAA, 2012
- [9] Sedhai, S., "*A Multiscale Flame-Embedding Framework for Turbulent Combustion using LES-ODT*", Master's thesis, North Carolina State University, 2011
- [10] Balasubramanian, S., "*Novel Approach for the Direct Simulation of Subgrid-Scale Physics in Fire Simulations*", Master's thesis, North Carolina State University, 2010
- [11] Kerstein, A. R., "*One Dimensional Turbulence: Model Formulation and Application to Homogeneous Turbulence, Shear Flows, and Buoyant Stratified Flows*", Journal of Fluid Mechanics, 392:277-334, 1999

- [12] Punati Kumar, N., *“An Eulerian One-Dimensional Turbulence Model: Application to Turbulent and Multiphase Reacting Flows”*, PhD thesis, University of Utah, 2012
- [13] Ricks, A.J., Hewson, J.C., Kerstein, A.R., Gore, J.P., Tieszen, S.R., Ashurst, W.T., *“A Spatially-developing One Dimensional Turbulence Study of Soot and Enthalpy Evolution in Meter-scale Buoyant Turbulent Flames”*, *Combustion Science Technology*, 182:60-101, 2010
- [14] Chapman, S., Cowling, T. G., *The Mathematical Theory of Non-uniform gases: an Account of the Kinetic Theory of Viscosity, Thermal Conduction and Diffusion in Gases*”, 3rd Edition, Cambridge University Press, 1970
- [15] Neufield, P. D., Jansen, A. R., Aziz, R. A., *“Empirical Equations to Calculate 16 of the Transport Collision Integrals for the Lennard-Jones (12-6) Potential”*, *Journal of Chemical Physics*,57:1100-1102, 1972
- [16] Poling, B. E., Prausnitz, O’Connell, J.P., *“The Properties of Gases and Liquids”*, 5th Edition, McGraw-Hill, 2001
- [17] McGrattan, K., Hostikka, S., Floyd, J., Baum, H., Rehm, R., *“Fire Dynamics Simulator (Version 5) Technical Reference Guide”*, NIST (National Institute of Standards and Technology), 2007
- [18] Puri, I., Seshadri, K., *“Extinction of Diffusion Flames Burning Diluted Methane and Diluted Propane in Diluted Air”*, *Combustion and Flame*, 65:137, 1996
- [19] Sobolev, S. L., Vaskevich, V. L., *“The Theory of Cubature Formulas”*, Sobolev Institute of Mathematics, Siberian Division of the Russian Academy of Sciences, Kluwer Academic Publishers, 1996

- [20] Press W. H., Teukolsky, S. A., Vetterling, W. T., Flannery, B. P., *“Numerical Recipes in Fortran”*, Cambridge University Press, 2nd Edition, 1996
- [21] Wesseling, P., *“Principles of Computational Fluid Dynamics”*, Springer-Verlag Berlin Heidelberg, 2001
- [22] Hanifi, A., Alfredsson, P. H., Johansson, A. V., Henningson, D. S., *“Transition, Turbulence and Combustion Modelling”*, Kluwer Academic Publishers, 1998
- [23] Pitsch, H., *“Large-Eddy Simulation of Turbulent Combustion”*, Annual Review of Fluid Mechanics, 38:453-482, 2006
- [24] Vervisch, L., Veynante, D., J. van Beeck, J.P.A., *“Turbulent Combustion, Lecture Series 2009-07”*, von Karman Institute for Fluid Dynamics, 2009
- [25] Smagorinsky, J., *“General Circulation Experiments with the Primitive Equations”*, Monthly Weather Review, 91:99-164, 1963
- [26] Meneveau, C., *“Turbulence: Subgrid-Scale Modeling”*, Scholarpedia, 5:9489, 2010
- [27] Werner, H., Wengle, H., *“Large-Eddy Simulation of Turbulent Flow around a Cube in a Plane Channel”*, Turbulent Shear Flows Symposium, Springer, 8:155-68, 1993
- [28] Piomelli, U., *“Wall-Layer Models for Large-Eddy Simulations”*, Progress in Aerospace Sciences, 4: 437-446, 2008
- [29] Hergert, W., Wriedt, T., *“The Mie Theory, Basics and Applications”*, Springer Series in Optical Sciences, 2012
- [30] Ma, T.G., Quintiere, J. G., *“Numerical Simulation of Axi-symmetric Fire Plumes: Accuracy and Limitations”*, Fire Safety Journal, 38: 467-492, 2003

- [31] Cao, S., “*A Novel Hybrid Scheme for Large-Eddy Simulation of Turbulent Combustion Based on the One-Dimensional Turbulence Model*”, PhD dissertation, North Carolina State University, 2006

APPENDICES

Appendix A

Tri-linear Interpolation

Downscaling the scalars from LES grid to ODT grid exploits tri-linear interpolation. These scalars addressed in the coupled LES-ODT methodology are mixture fraction and velocity [20], [21]. These scales are resolved by LES governing equations. In a sense, downscaling the scalars stands opposite to filtering and upscaling the information.

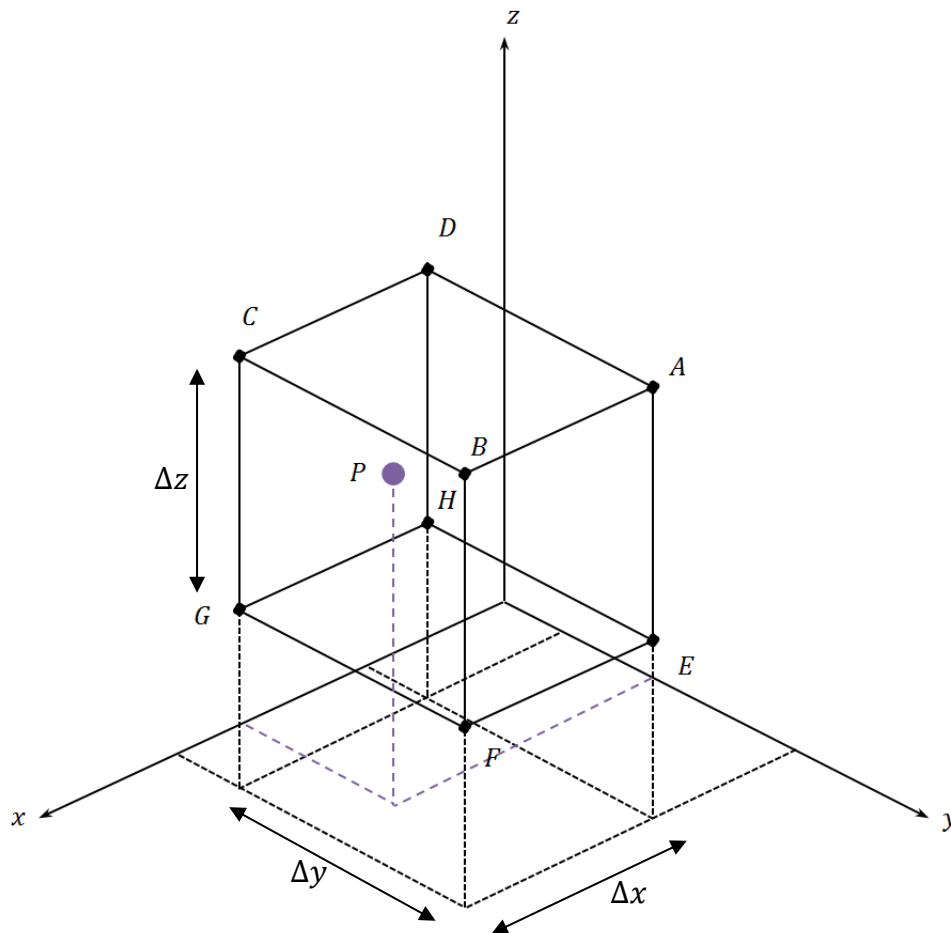


Figure A.1 Tri-linear interpolation for a cell

In the prism above, it is assumed that each node has an assigned value. If point $H(x_0, y_0, z_0)$ were tagged with index (i, j, k) , then $\varphi_{i,j,k}$ would be the corresponding values at node H . To interpolate the value at arbitrary point $P(x_p, y_p, z_p)$, within the cell above, method of tri-linear is used. The cell can be divided in to 8 volumes by planes defined by $x = x_p, y = y_p, z = z_p$. These volumes can be normalized by dividing them by the total volume of the cell.

$$\lambda_1 = \frac{x_p - x_0}{\Delta x} \quad (\text{A.1})$$

$$\lambda_2 = \frac{y_p - y}{\Delta y} \quad (\text{A.2})$$

$$\lambda_3 = \frac{z_p - z_0}{\Delta z} \quad (\text{A.3})$$

$$\begin{aligned} \varphi_p = & \varphi_{i,j,k}(1 - \lambda_1)(1 - \lambda_2)(1 - \lambda_3) \\ & + \varphi_{i+1,j,k}(\lambda_1)(1 - \lambda_2)(1 - \lambda_3) \\ & + \varphi_{i,j+1,k}(1 - \lambda_1)(\lambda_2)(1 - \lambda_3) \\ & + \varphi_{i,j,k+1}(1 - \lambda_1)(1 - \lambda_2)(\lambda_3) \\ & + \varphi_{i+1,j+1,k}(\lambda_1)(\lambda_2)(1 - \lambda_3) \\ & + \varphi_{i+1,j,k+1}(\lambda_1)(1 - \lambda_2)(\lambda_3) \\ & + \varphi_{i,j+1,k+1}(\lambda_1)(\lambda_2)(1 - \lambda_3) \\ & + \varphi_{i+1,j+1,k+1}(\lambda_1)(\lambda_2)(\lambda_3) \end{aligned} \quad (\text{A.4})$$

Appendix B

Note on Spatial Filtering

Here the basic concept and its formulation are proofed.

Imagine line ℓ in 3D space, represents the ODT element attached to the flame surface. The procedure is set based on finding the distance of the LES cell center and the ODT element. The foot of the perpendicular PI on the line can be obtained. The corresponding distance of each LES cell center to the ODT grid point the element is calculated. Note that the line has a normal vector, \vec{n} and can be obtained from the corresponding stoichiometric mixture fraction.

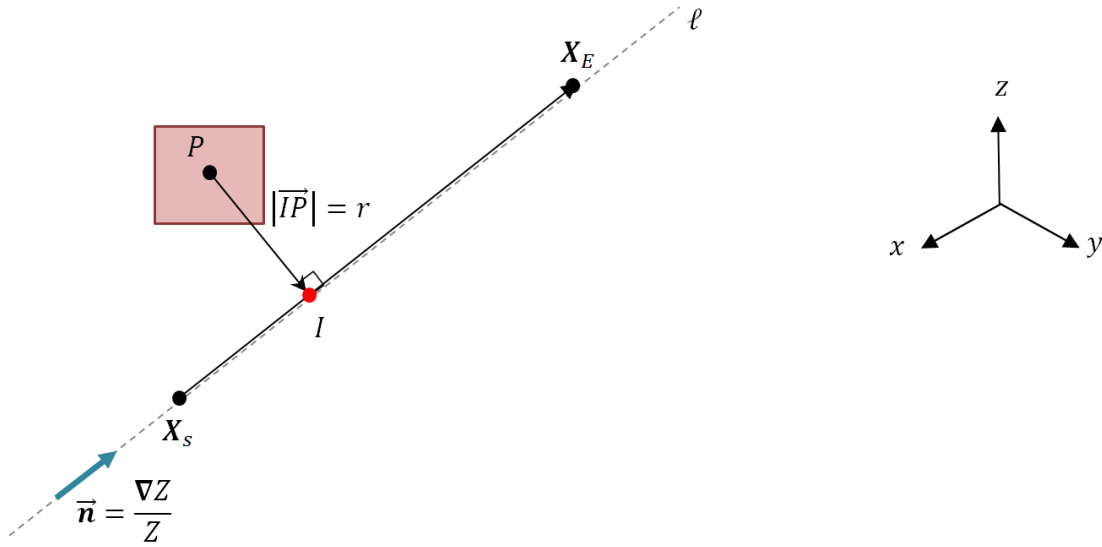


Figure B.1 Finding distance between LES cell center and ODT element

$$X_S = (x_{min}, y_{min}, z_{min}), X_E = (x_{max}, y_{max}, z_{max}) \quad (B.1)$$

$$L_{ODT} = |\overrightarrow{X_S X_E}| \quad (B.2)$$

$$\vec{n} = \vec{n}_1 + \vec{n}_2 + \vec{n}_3 \quad (B.3)$$

$$n_1 = \frac{(x_{max} - x_{min})}{L_{ODT}}, n_2 = \frac{(y_{max} - y_{min})}{L_{ODT}}, n_3 = \frac{(z_{max} - z_{min})}{L_{ODT}} \quad (B.4)$$

$$\ell: \frac{x_{max} - x_{min}}{n_1} = \frac{y_{max} - y_{min}}{n_2} = \frac{z_{max} - z_{min}}{n_3} \quad (B.5)$$

$$\vec{PI} \cdot \vec{X_S X_E} = 0 \quad (B.6)$$

$$(x_i - x_p) \cdot (x_{max} - x_{min}) + (y_i - y_p) \cdot (y_{max} - y_{min}) \quad (B.7)$$

$$+ (z_i - z_p) \cdot (z_{max} - z_{min}) = 0$$

Also: $I \in \ell$

$$y_i = (x_i - x_{min}) \left(\frac{n_2}{n_1} \right) + y_{min} \quad (B.8)$$

$$z_i = (x_i - x_{min}) \left(\frac{n_3}{n_1} \right) + z_{min} \quad (B.9)$$

Inserting (B.8) and (B.9) into (B.7) yields x_i . Hence, the foot of perpendicular point is known.

$$r = |\vec{PI}| = \sqrt{(x_i - x_p)^2 + (y_i - y_p)^2 + (z_i - z_p)^2} \quad (B.10)$$

$$r^* = \frac{r}{\mathcal{R}_{eff}} \quad (B.11)$$

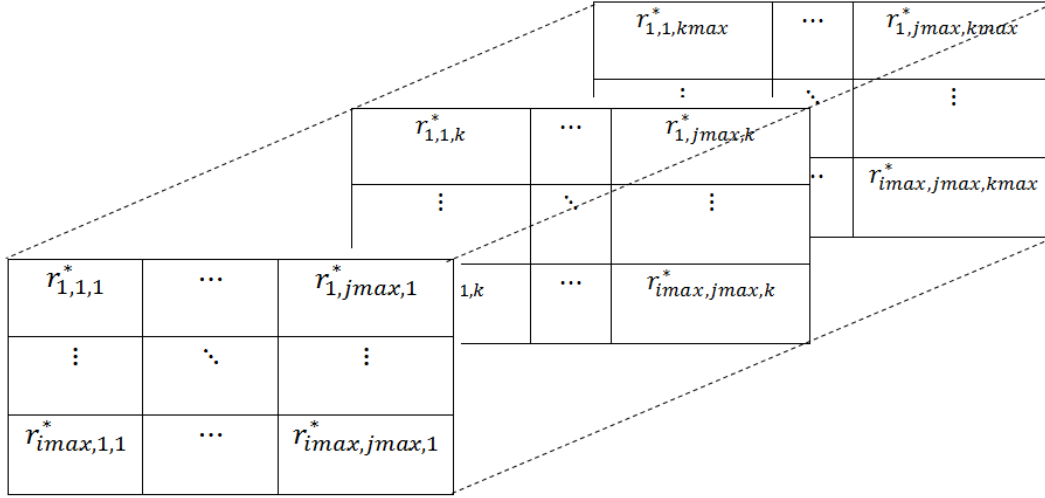
If the resolution of the ODT domain is denoted by M and the number of the domains by N , then ODT density can be represented as follows:

$$\rho_{ODT} = \begin{pmatrix} \rho_{11} & \cdots & \rho_{M1} \\ \vdots & \ddots & \vdots \\ \rho_{1N} & \cdots & \rho_{MN} \end{pmatrix}$$

Corresponding to the 3D LES grid, a 3D array, $R_{i,j,k}^l$ can be defined for the dimensionless radius, r^* . Note, i, j, k determines the location of the LES cell and l as superscript shows the

specific ODT domain which the distance is calculated. This array is used to find the weighting of each ODT domain in each adjacent LES cell centers.

This array $R_{i,j,k}^l$ for the ODT number l can be written as:



Corresponding to $R_{i,j,k}^l$, an array $W_{i,j,k}^l$ can be defined based on Gaussian Cubature Method for each LES cell. The accumulated weight and density for each cell is computed.

$$w_{i,j,k} = \sum \exp\left(-\frac{r_{i,j,k}^{*2}}{\sigma^2}\right) \quad (\text{B.12})$$

Hence,

$$\bar{\rho}_{i,j,k}^{LES} = \left(\sum_{LES \text{ Cell}} \rho_{m,n} w_{i,j,k}(\mathbf{r}^*) \right) / \left(\sum_{LES \text{ Cell}} w_{i,j,k}(\mathbf{r}^*) \right) \quad (\text{B.13})$$